Feedback Controlled Variable Electric Field System for Smart Contactless Gripper.

BY

MALIK AQIB REHMAN

01-244172-013

SUPERVISED BY

DR. SAYED ASIM ALI SHAH

Session-2017-2019

A Report submitted to the Department of Electrical Engineering

Bahria University, Islamabad

in partial fulfilment of the requirement for the degree of MS(EE)

CERTIFICATE

We accept the work contained in this report as a confirmation to the required standard for the partial fulfilment of the degree of MS (EE).

_____	_____
Head of Department	Supervisor
_____	_____
Internal Examiner	External Examiner

DEDICATION

I dedicate this dissertation to my lecturers/faculty members who have supported me throughout the process. I am very thankful to my parents who gave me both the moral and financial support needed to achieve the milestone.

DECLARATION OF AUTHORSHIP

I hereby declare that content of this thesis is my own work and that it is the result of work done during the period of registration. To the best of my knowledge, it contains no material previously published or written by another person nor material which to a substantial extent has been accepted for the award of any other degree or diploma of the university or other institute of higher learning, except where due acknowledgement has been made in the text.

Parts of this thesis appeared in the following publications, to each of which I have made substantial contributions:

- Publication…

_____

(Student Signature)

ACKNOWLEDGEMENTS

I greatly thankful to my supervisor Dr. Syed Asim Ali Shah who has provided me with a very thorough assistance and a persistent support throughout the research work.

ABSTRACT

Variable electric field has a large amount of applications nowadays, which is used in automation in industry. Minimization of the hardware at all levels in automation and industry are the key important which are important to increase the usefulness and productivity of all system. One of the applications of electric field is in Van de Graff generator. Electric Field is also used to measure cell and tissue properties. In this research work presented here is based around the development of a fuzzy based feedback controlled variable electric field system using HFO. This research is central to advanced industrial applications like contactless gripper, ion implantation and silicon chip placement. We have developed a system that is able to generate, control and monitor variable electric field. The developed system is capable of producing variable fields and the proposed system can be implemented in many dynamic environments. The designed system also monitors and measures the field produced by the developed electric field generator. Developed model has been executed on simulation tools. After finalization of design parameters, hardware of the system has been developed. The developed hardware has the capability of generating variable Electric Field using solid state tesla coil. Sensor for field measurement has been incorporated by using National Instruments DAQ USB 6001. The same sensor provides feedback to controller which controls, monitors and updates the field according to the user's requirement.

CONTENTS

LIST OF FIGURES

LIST OF TABLES

ABBREVIATIONS

EF	Electric Field
PWM	Pulse Width Modulation
PFM	Pulse Frequency Modulation
HFO	high frequency oscillator
FO	Field offset
DC	Duty cycle
FBG	Feedback gain
K	Gain
SO	System offset
AMR	Anisotropic Magneto Resistance

Chapter 1

Introduction

CHAPTER 1. INTRODUCTION

1.1. Thesis Background/Overview

A control system has the capacity of commanding, supervision and amendable other devices with the help of control loops. Every component and element connected to the system has an impression of its own on the output. The basic determination of the system design is to be able to acquire and generate the required output.

Control System Engineering makes sure that there is a well-designed and a very organized method to increase productivity and to assist a fast growth of control industry. The main purpose of the control systems is to minimize incompetent manual controls in this manner eradicating the human errors and efforts that would protect company prosperity.

With the swift transformation of the human development the need to automate the systems has ascended exponentially. In the critical verge period control structures assume a remarkable part in the development and association of the most recent improvements and henceforth the human development. Each part of our regular day to day survival has been affected by the control structure. Ventilation and cooling system, a cutting edge vehicle, a hot water geezer, and a programmed printing press are all the usual utilizations of control system strategies. The control frameworks envisioned for the mechanical utilize to deliver more yield as they work at the most important amount of precision. Control frameworks are similarly utilized as a part of

the quality control of the products. They are also used to produce robots, weapons, space innovations transportation and almost in every field of modernized world.

Electric field is a force of field that surroundings electric charges that draws or repels other electric charges in its surroundings. Electric fields are produced by electric charges and time changing magnetic fields.

Electric fields have been a very important part of many industrial applications which we will be the main focus of our research. We will develop a system that will be able to generate variable Electric Field, control and monitor that field. The generated electric field would be capable of generating static and variable charges and could be employed in a dynamic environment. The designed system will also monitor and measure the electric field produced by the developed system.

First of all we developed the hardware design that have the capability of generating variable Electric Field by the use of tesla coil and high frequency oscillator. Then we have incorporated Hall Effect and current Sensor to measure the generated electric field and provide the feedback to the controller through National Instruments Data Acquisition Card. Then the measurement & controlling of Electric Field will be done on LABVIEW Software.

An input ranging from 2T to 5T will be given to the DAQ card using the software programme which will then send the input data to the solid state tesla coil to generate the required electric field. A hall effect or current sensor will ensure that given input is generated by the tesla coil. The sensor will detects if the required field is not being generated then it will readjust its value using feedback control loop and high frequency oscillator on a feedback mechanism will ensure the generation of required

five tesla electric field. Hence the system will be fully feedback controlled. Signal conditioning and filtering is also being done using LABVIEW software to remove noise and attenuation from the signals.

1.2. Problem Description

- To design & develop a Fuzzy based feedback controlled variable Electric Field System using HFO with the capability of generating, monitoring and measuring the electric field produced through this system.

1.3. Thesis Objectives

- Circuitry capable of generating Electric fields of variable intensity.
- To develop feedback controlled variable electrical field generator.
- Development of fuzzy based strategy to effectively adjust the electric field according to predefined value.
- To design a software program which will have the provision to control and monitor the electric field.

1.4. Project scope:

Robotic arms these days have a very dynamic role in industrial automation. In many industrial industries the robotic arms are mainly used for tasks where robotic gripper manipulates the objects from one point to another point. Main applications of robotic

arm includes in palatalizing process in which components are arranged in order for the purpose of packaging or feeding to a machine. Another important application is set up in car and automobile industry where such robotic arms are used mainly for welding different parts. These industrial robotic arms are mainly used in versatile environments where there is a high chance of danger and safety issues to humans. Robotic arms are also increasingly used in different assembly processes of different components in industry. Another big and most benefiting application of robotic arms is in medicine / surgical industries for the production of various surgical / medical equipment where there is a high chance of bacterial contamination that is not acceptable in any circumstances. Designed project will be a great breakthrough in field of contactless grippers.

Chapter 2

Literature Review

CHAPTER 2. LITERATURE REVIEW

A lot of work has been done in the field of generating electric fields for vast applications for example medical industry, food preservation and silicon chip manufacturing. Some related research work is studied and stated here.

2.1. Electric Field:

Electric field is a force of field that includes electric charges that pulls towards or pulls away further electric charges. Precisely the electric fields are the vector field that associates to every point in space the power called the coulomb force that can be sensed per unit of the charge. The Standard International units of the electric field are N/C where N stands for Newton and C stands for coulomb or V/m where V stands for volts and m stands for meter. Electric charges with the time-varying fields make up the Electric fields.

2.1.1. Tesla Coil:

A tesla coil was first invented by Nikola Tesla in 1892. Tesla coil is an electrical resonating transformer that can produce high voltage with low current and high frequency AC signals. It is a frequency oscillator that runs an air-centre two fold tuned thunderous transformer to deliver high voltages at low streams. Tesla's remarkable circuits and most current coils use a clear begin opening to stimulate actions in the tuned transformer. [1] A typical tesla coil can produce voltages ranging from 40 kilovolts to millions of volts for wide loops.

2.1.2. LABVIEW software:

LABVIEW is a software platform of frameworks providing user to build programming algorithms for versatile applications and designs that require testing, valuation, and to conqqtrol with fast access to equipment, components and information bits of knowledge.

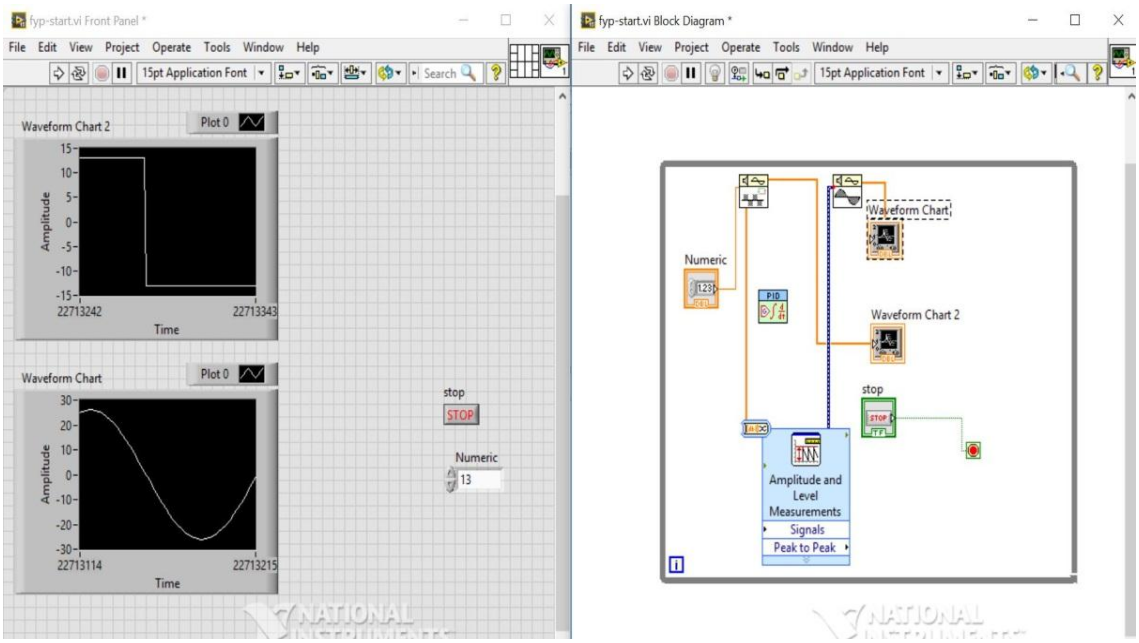

Fig 2.1:A basic demonstration of interchanging different waves in LABVIEW software

2.2. Previously Existing Methods

2.2.1. Van de graaff generator:

A Van de graaff generator is an electrical instrument that can generate electrostatic charges. Van de graaff comprise of a moveable belt to collect electric charge on the surface of hollow metal globe on the topmost of an insulated column like structure generating very high electric potentials [2]. This apparatus can yield very high

voltage, direct current DC electricity at small current. Van de graaff generator was first invented Robert J. Van de graaff in 1929.

A van de graaff generator can generate voltage of different magnitudes. A pointed metal brush had been given positive charge by a power supply that runs by a help of pulley [3]. Electrons are ejected from the belt leaving it in a state of being positively charged. A similar brush placed up permits the remaining positive charge to spread on to the dome.

Van de Graaff generator consists of a moving belt on more than two rollers of opposite materials one of the rollers exists fused by an empty metal circle dome. Two terminals as brushes formed columns of very sharp metal centres are located close to the base of the lower roller and in the circle over the upper roller. A comb shaped structure is linked with the circle dome and another one to the ground. The scheme for charging depends on the turboelectric impact with the goal that forthright contact of two distinctive materials for the interchange of a few electrons from one material to the next material. The elastic belt will try out to be charged however the acrylic glass of the upper roller will turn out to be definitely charged. The belt entertains negative charge on its internal surface while the upper roller collects positive charge. Next the solid electric field surrounding the positive upper roller provokes a high electric field close to the purposes of the close by brush. On the concentrations the field winds up necessarily solid to ionize the air particles and the electrons are dragged in to the outside of the belt whereas positive particles go to the brush [4]. At the brush they are executed by electrons that were on the brush along these lines leaving the brush and the connected to external shell with less net electrons. The plentiful positive charge is gathered on the external surface of the external shell leaving the inside of the cell

deprived of any field. This technique helps Electrostatic induction develop a lot of charges on the shell.

Fig 2.2:A 500,000 V Van de Graaff generator.

2.2.2. Pulsed electric field Generation:

Pulsed electric field generation technique is utilized in cell splitting of the tissues of different life forms which repairs massive transport structures and improves product quality for a widespread scope of applications.

The Pulsed electric field progress yield extraordinary power electric fields to give a non thermal handling to whipping the pathogens and attaining a massive decrease in the number of the micro-organisms impacting food products in food industry. The product's life time span of usability for practical ease of use is prolonged with no undesirable effect caused by the mainstream warm systems; i.e pasteurization. This development delights the product in its capacity and not only the surface. It is particularly reasonable for the liquids.

Regarding the development the hardware involves a cell where the liquid to be managed is kept between two anodes which will be the metal plates in our case related with the high voltage pulse generator. The impulse frequency rest on the liquid stream speed. Voltage compel associated depends upon the division between the metal plates and the current on the liquid conductibility. The treatment traverse may be satisfactory to deactivate the micro-organisms.

The voltage generator is designed of extensive high voltage capacitors, one voltage supply charging every one of the capacitors and one to the high voltage switch interfacing the capacitors to the anodes in the cell for term of the impulse [5]. The electric field in the cell is being calculated using: E = v/d. where v = voltage between the electrodes. d = separate among the terminals.

2.3. Related work.

Different researches had been carried out on generation of electric field and variety work has already been done on the generation of static Electric Fields. Some of the research papers were analysed and summarized here.

High power magnetron work with the postulation that cathode can endure extreme temperatures and high electron attack. In this research a kind of variable field helical cathode is presented so as to weaken the focal part temperature of cathode in magnetron and afterward increase its lifetime. Its electrostatic field stability is represented by CST-EM and compared with the tube shaped cathode and helical cathode [6]. The effects demonstrate that variable pitch cathode surface electric field has a little change moreover its consistency resembles even pitch cathode. With the

expansion of radius the consistency enhances and it is near the tube-shaped cathode. So it might be incorporated in magnetrons to enhance magnetrons execution and broaden their lifetime.

The interconnection of spontaneous components, sensor chips and actuators on a usual silicon substrate over micro chip fabrication technology is called a MEMS structure or assembly. MEMS mark the evolution of the Integrated Circuit industry. The above technology has inherited several features from its parent Integrated Circuit technology. Some of the inherited characteristics include compactness, microelectronics integration and accurate bunch production. This technology sanctions for the fabrication of devices as small as 1 micro meter. A big attention is given to the mechanical behaviour of a gold diaphragm tuner's contraction. The deflection of the diaphragm tuner is primarily caused by electrostatic force between the diaphragm and dc biasing electrode. An increase in the input power causes radio frequency to effect the electrostatic forces in a way as to deflect the diaphragm. This phenomenon causes the diaphragm to be pulled towards the capacitive post which in turn results in a non-linear response. The system is then modelled on the COMSOL software as well. The model is made to simulate and analyse all the possible results of the experimentation. The end results suggest that the substrate properties of transposition of diaphragm and potential have no effect on the electrical field distribution of the system [7]. The claim has further been strengthened by the graphical evidence provided. It can be safely concluded that changing substrate properties simply effects the electric field sharing. Rest of the factors remain unaffected.

Yotsuyanagi, H., et al have discussed about the mostly occurred faults which come in the shape of short and open circuit in IC's. These faults appear to be insignificant but cause major defects and problems in results and are difficult to be detected. In this research paper author has proposed a new methodology to find open circuit IC fault in the circuit. System will take place in such a way that variable time electric field will be provided and in case of open IC excessive current will flow and will flow through a conducting path. Circuits with open ICs have floating node and when electric field is applied to that circuit it causes a change in voltage on node. Procedure is explained by the help of example. In this examples author explains that faulty IC's were detected by the help of sine waves a large amount of current was found in defected IC circuit [8]. For further conditions more examination is required. Authors conclude that they have presented a new method for detecting opens and have shown us random pattern testability of this method. According to them their test method can give 100% results because fault propagation to the primary output is not necessary. But still a deterministic pattern for this test is required.

The preservation of food using the pulsed electric fields is unique of the most favorable non thermal processing methods. Jeyamkondan et al. has presented a brief review by analyzing the various methods of food preservation from the inactivation of a microorganism [9]. When Pulsed Electric Field was applied to the cells the cell membrane was disrupted which resulted in the leakage of intercellular contents of the cell and hence preservation was carried out by making them inactive.

Tsuruda et al. designed the equation **E + V x B = 0** to relate the global motion of plasma in the magnetosphere perpendicular to the magnetic fields and the electric fields. Particles acceleration mechanism is the most important targets in the magneto-

spherical study which require the presence of electric field [10]. Highly reliable measurements of the electric fields play critical roles in the magneto-spherical research.

Jones et al. used the electric fields for the levitation of minor metallic particles in insulating dielectric fluids. Levitation was attained by injecting the particles to be rise up into a cell through a hole in the subordinate electrode. Non-uniform electric fields were used to attract particles to the upper electrode [11]. As voltage dropped to zero due to the activation of the feedback control system, the absence of electric field detached the particles from the higher electrode and dropped them in to the region wherever an optical system was placed to detect the particle's position in the region.

Paraliev et al. used electric field to design an electron gun for the X-ray Free Electron Laser applications (XRFEL) [12]. To achieve low emittance, the electron gun utilized field radiation and great accelerating gradient.

Ronnie et al. tested electromagnetic field senor system by a moving artificial field source and an electric field sensor equipped Autonomous Underwater Vehicle (AUV) [13]. The focus of the work was to determine the effectiveness of the electric field sensors equipped to AUV to accurately measure electric field in the ocean environments. When the accuracy of AUV position was known to be within ~1 m, the peak value of AUV obtained at the closest pass was consistent with the predicted field of the artificial source.

A J Young et al. developed a prototype high power system capable of producing high intensity electric fields impulses in medical applications. A pulsed power system was realised from a pair of equivalent connected 200 μF/22 KV capacitors. Reverse

charging was prevented by a parallel connection of a reversed biased 10 diode stack and a ballast resistor. The magnetic coil system was jointed to the power supply by five parallel connected 10m long high voltage cables. Rogowski coil monitored the coil current. An accurate prediction of inductance of the double coil system and electric and magnetic fields produced using 2-D modelling of the magnetic field distribution enabled the overall system to be optimised [14]. Multiple shots at 15 KV were sustained by the coils.

J.H.Woo et al. detected a Pancharatnam's phase of light via liquid crystal cell. The distinctions in the inquisitive pattern were examined in relations of the geometric phase variation [15]. The occurrence of geometric phase jump exhibited the electric fields dependency of the interference configuration alteration. By varying refractive index and angle of the optic axis of liquid crystal cell a particular behaviour of interference pattern was observed which was initiated by the change in behaviour of geometric part [17].

However, these electric fields are applicable for robotic arms being utilized as manipulators [16]. Various mobile robots utilizes such robotic arms as end effectors. These mobile robots are being incorporated in various human service areas such as in departmental stores as shopping cart or as assistant in hospitals etc. Such robots perform Human Robot interaction and are being used to provide service to human beings [18].

2.4. Electric Field Measurement

The electric fields scattering by using the Kerr effect method in dielectric liquid was thoroughly investigated by Z. N. Zakaria et al. [19]. In the experiment the electrodes system was realized by the application of parallel-plane under DC electric field. A detector recorded the light concentration images of the transmitted light from the laser beam. The work was focused on determining the relationship between the transmitted light intensity and the electric fields applied to the system. The comparison of images obtained between the incident light intensity and concentration of the transmitted light over the technique of image enhancement showed that the intensity was uniformly dark when there is no electric field, but upon the increase in electric field, the intensity ratio of incident light to transmitted light also increases. F.S Mozer et al. [20] measured the horizontal and vertical electric fields by flying two balloons. During magnetic bays, ground-based magneto meters principally measured Hall currents whose variations depended on conductivity changes as much or more than on electric field variations. For a period of about 30 minutes before the start of a negative bay near indigenous midnight, the ionosphere electric fields pointed westward indicating radially internal flow in the equatorial plane [46-59]. These results were interpreted in terms of a model of the magnetosphere sub storm in which inlets are triggered deep inside the magnetosphere by a variability associated with a radial plasma density gradient established by convective flow. The average electric fields in dayside ionosphere were smaller than the electric field at night, which proposes that the dayside magnetosphere co-rotate with the earth.

2.5. Electric Field Generation

Xavier et al. used two equal biconical electrodes of equivalent and differing potential values to form a system for identical electric field generation [21]. This method was used for the calculation of the potential and fields of the observed system because of its easiness and accurateness. Homogeneous electric fields existed in the fundamental region of electrode system when angular width of conical electrodes was chosen so that $\alpha = \alpha 0 = \text{actg}\ \sqrt{2}/3 \approx 39.2315^{0}$. L. Richard Huang at al. [22] introduced a new method for producing tuneable even electric fields over huge micro fluidic arrays in 2D and its uses to a micro fabricated devices which is used to separate genomic DNA. The system made use of current injection method over orthodox electric potential to define electric fields. A single lithographic process can easily micro fabricate the current sources. Problems of bubble generation and electrode erosion did not occur because no electrodes are used. The implementation of the method was made practical by the small number of voltage contacts used. Uniform electric fields were obtained because of the use of large number of resistors. The DNA was delivered and extracted to and from the array using the channels. Current injection method's compatibility with the lab on chip devices made it useful for many real-world micro fluidic applications.

2.6. Electric Field Control

The uses of electric fields can differ the conductivity of semiconductors, however its impact on magnetism has proved indefinable. The research work carried on by H.Ohno et al. [23] focused on the demonstration of electric field controller of Ferro magnetism in a skinny thin film semiconducting alloy using an insulating-gate field effect transistor formation. The application of electric fields allowed varying the conversion

temperature of hole induced Ferro magnetism isothermally and reversibly. These holes aided magnetic interactions, bring about ferromagnetism. Since a weak anti Ferro magnetism caused by super exchange was seen without holes, the diminishing (increment) of holes deliberation by the utilization of electric fields brought about a lessening an increase of the hole facilitated ferromagnetic interchange association among confined Mn spins and thus in adjustment of ferromagnetic properties. The total phase can be intended as a function of δ. Shizu Wu et al. [24] designed Ta/NiFe/BiFeO3 (BFO)/SrRuO3/SrTiO3 heterostructure by the pulsed laser disintegration and magnetic gasping. The BFO film is unadulterated and exceptionally arranged. Run of the mill anisotropic magnetoresistance (AMR) impact was detected by four tests procedure at standard room temperature. While smearing an out of plane electric field, noticable inverts of the AMR stage were seen a few times from about −0.015% to around 0.015% in the examination. The outcomes showed that a reversible electric fields control in ferro magnetic deposit can be generated through multi ferroic BFO at the room temperature. Food treatment is handled using thermal or non-thermal techniques. Barba et al. [25] invented a method of microbial deactivation in food using Pulsed Electric Fields (PEF).

2.7. Fuzzy Based Control

Omrane et al. used Fuzzy based systems to develop performance based control of a mobile robot for responsive navigation [26]. The designed Fuzzy system renovates sensors input to obtain wheel speeds. Handcrafting, a technique based on the optimal generation of training sequence, was used for the generation of Fuzzy system's rule bases. The simulations results obtained of the navigation using fuzzy based mobile

robot navigation systems show good performance in complex and unfamiliar environments. Lakhmi et al. designed two dimensional fuzzy descending mode control of a field sensed magnetic suspension system [27]. System employs the use of fuzzy set of rules which contain both sliding assorted and its derived. The new design circuits implemented simple, inexpensive and effective driver, sensor and control circuits. To develop a better profile for the electricity consumption, a methodology was presented by Ahmed et al. which was used to gain genetic fuzzy rule based systems under the iterative rule learning approach MOGUL methodology [28]. The approach makes use of the past hours to estimate the intake value of the given hour. The approach employed is more trustworthy and all the planned errors are closer to the normal error. Aerodynamic modelling of the fixed aircraft was introduced by Singh et al. as an application of fuzzy logic. Stability derivatives and rolling moment control of ATAS air craft are obtained from documented flight data of nonlinear flight contour for the demonstration of the above model [29]. A nonlinear dynamic of aircraft is represented using fuzzy logic based TSK model. Liu et al. made use of the fuzzy logic control to demonstrate the optimization of light tracer movement. A dual axis type which can follow the light in both the directions was used in the light tracking system [30]. A light senor is mounted on the solar tracker to compare light intensity at each point. Results suggested that fuzzy logic method is more suitable to be implemented in light tracking system as it is smoother compared to the non-fuzzy methods. Syamsul et al. present the application of fuzzy logic based governor in purification procedure of nut meg oil [31]. The governor system was built on the foundation of fuzzy logic with two main parameters of temperature and vapour pressure. The maximum optimum value of the fuzzy logic model was then rooted to

the micro controller to regulate the location of the gas movement valve. The fuzzy logic based control system is capable of reducing the purification time from 24 hours to 16 hours on average. Febryan et al. proposed the design and improvement of a fuzzy logic based server room temperature as well humidity control which made use of wemos D1 as an ultraviolet transmitter remote control for the temperature regulatory purposes as well as modes setting for Air conditioner to keep the humidity and temperature in the server room in control [32]. M. Fedorová et al. demonstrated the probable of the fuzzy system method to analysis of health care catalogues for clinicians in their repetitive daily exercise [33]. The fuzzy scheme method was functional to the analysis of medical instruction items for I 10.90 and E 11.90 comorbid patient as the most regularly identified cardio vascular and endocrine codes of analyses [35-45]. The outcomes of this study propose that the fuzzy system approach to health care data attained from insurance companies might be a cooperative way of producing information useful for final conclusion process in the drugs assortment for similar poly morbid patients in medical practice.

2.8. Existing Systems

There already exist numerous ways of generating static Electrical Fields.

2.8.1. Holtz machine:

During the 1870's, Holtz assembled and portrayed a broad number of impact machines which were seen as the most dynamic progressions of the time. Fit as a fiddle, the Holtz machine included a glass hover fixed on a level center point which

could be made to turn at an enormous speed by a dual gear, speaking with enrollment plates mounted in a settled hover around it. Previously Toepler had developed an impact machine that included two plates settled on a comparable shaft and turning a comparative way. Following the trend the Schwedoff developed a machine that had a curious structure to manufacture the yield current. Similarly, a couple of mixed rubbing sway machines were created, including the Kundt machine and the Carre machine. Just before Holtz, H. Julius Smith acquired the American patent for a minimized and hermetically fixed instrument that was expected to light powder. Furthermore during the same yeras, sectorless machines in Germany were investigated by Poggendorff.

2.8.2. Wimshurst machine:

The Wimshurst machine is an extensively basic machine; it works, as all impact machines, with electrostatic enlistment of charges, which implies that it utilizes even the scarcest existing charge to make and collect more charges, and rehashes this procedure for whatever length of time that the machine is in real life. Wimshurst machines are made out of: two protected circles connected to pulleys of inverse revolution, the circles have little conductive (generally metal) plates on their outward-confronting sides; two twofold finished brushes that fill in as charge stabilizers and are likewise where acceptance happens, making the new charges to be gathered; two sets of gathering brushes, which are, as the name suggests, the authorities of electrical charge delivered by the machine; two Leyden Jars, the capacitors of the machine; a couple of anodes, for the exchange of charges once they have been adequately aggregated. The straightforward structure and segments of the Wimshurst Machine

settle on it a typical decision for a custom made electrostatic trial or show, these qualities were factors that added to its prominence, as already specified.

2.8.3. Comparisons:

Keeping in view these generators in any case corona expulsion from revealed metal portion at high levels and poor protection results in diminished voltages. Their effectiveness is poor, appeared differently in relation to the mechanical effort which is required to convey electrical vitality. A typical electrostatic generator ensures that the degree of charge carried forward current to the high potential voltage cathode is low. Afterward the machine is active voltage measured at the terminal anode will increase till the spillage current after the cathode matches the rate of charge carriage. Along these lines spillage from the terminal chooses the best voltage achievable. van de graaff generator ensures that its strap permits the vehicle of dash into within significant vacant tube shaped cathode. This is perfect form to limit outflow and corona discharge so the van de graaff generator can deliver the finest voltage. This is precisely the reason that the van de graaff setup have been used for very electro static subdivision accelerating catalysts. In short greater the measurement the smoother the sphere is the further the voltage that can be achieved. Unfortunately van de graaf generator cannot efficiently maintain the produced electric field for longer periods; which is the requirement of our final project.

Chapter 3

Methodology

CHAPTER 3. METHODOLOGY

System design and development techniques are elaborated in this chapter. Simulations are performed on software Lab View.

3.1. System over view:

Proposed system is based on hardware as well as software part. Tesla coil circuit is designed to generate the electric fields. Tesla coil is being controlled by two techniques that are PWM and PFM. Proposed system is tested on these two different techniques. PFM technique is achieved by incorporating HFO circuit.

The Hall Effect sensor is utilized for measuring and sensing of field so that required field is being generated according to user defined values. The sensor is incorporated in feedback loop.

The fuzzy based controlled strategy is implemented because of the non-linearity of the tesla coil. The generated electric field is adjusted with the fuzzy logic parameters to make sure the accuracy of the system. The Lab View software is utilized for development of the proposed system because controller used in this system is DAQ card 6001 which is highly adaptive with fast response and durability. This software also helps to develop Graphical user interface which is user friendly.

3.2. Proposed System

The overall proposed system is shown in fig 3.1.

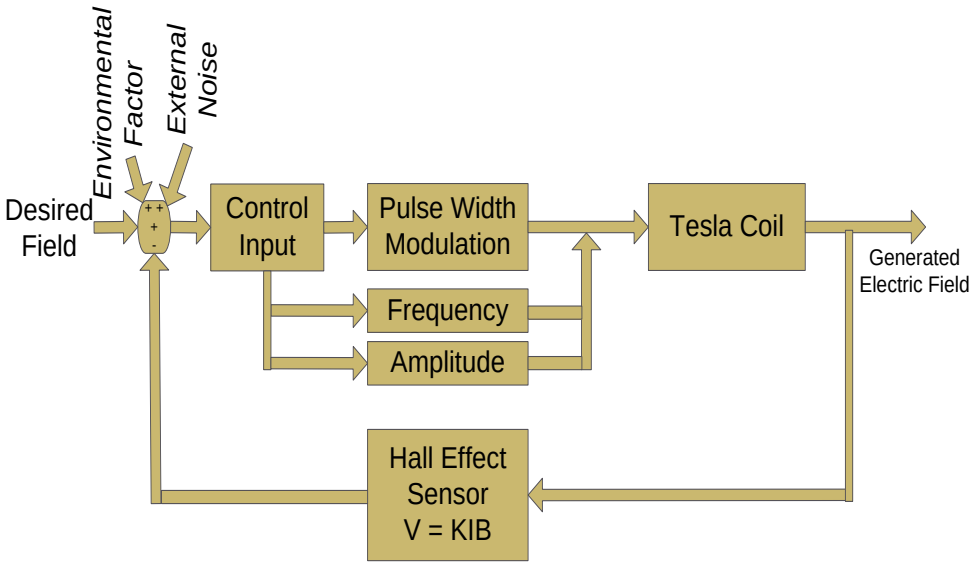

Fig 3.1: Controller Feedback Loop.

3.2.1. Variable Electric Field (VEF) Generation

The VEF system comprises of a Tesla Coil based circuitry for electric field generation along with a High Frequency Oscillator (HFO) circuit to input the high frequency signals to the Tesla Coil. The system will generate the required electric field & apply the control loop to adaptively adjust the field using fuzzy logic.

3.3. System Flow Strategy

In our system, NI DAQ is used as a controller. Tesla coil is used for the electric field generation. Hall Effect sensor which is the feedback sensor is used to measure the electric field. Sensor sends the data in feedback to the controller where fuzzy set of

rules readjusts the required electric filed and output is displayed on the user interface. An input is given to the DAQ card through NI Lab View. The input from DAQ card is given in the form of Pulse Width Modulation (PWM) signal later on this strategy is changed to High frequency Oscillator. Tesla coil generates the field given after receiving the input through Lab view program. Feedback sensor senses the electric field generated by the tesla coil. The same feedback is provided to NI DAQ & the lab view program decides the next command based on the fuzzy set of rules according to the system error. The flow of the system has been demonstrated in the Fig. 3.2.

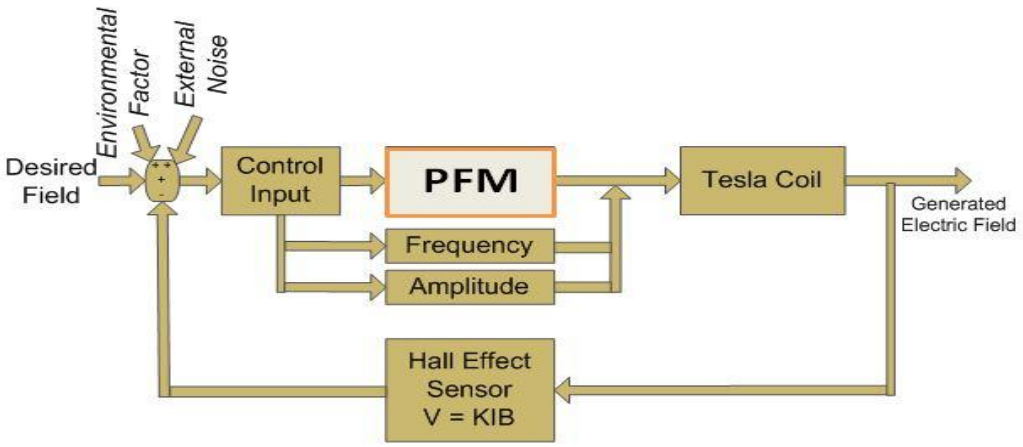

Fig 3.2: System block diagram

At first the signal is calibrated and integrated with hardware. Then we incorporated Hall Effect Sensor to measure the generated electric field and provide the feedback to the controller through NI DAQ. Then the measurement & controlling of Electric Field was done on LABVIEW Software.

Initially we designed a tesla coil that was pulsed using the 555 timer IC. Later on, it was realised that for generation of electric field ranging from 1.2T to 2.4T a

redesigning of tesla coil was required. Therefore Tesla coil was redesigned and the system has been operated using PWM command from DAQ card.

3.3.1. Using Fuzzy Logic

A fuzzy based system was then developed which includes the fuzzy set of rules. Block diagram of the fuzzy based system has been presented in Fig. 3.4. For this major stage of experimentation three basic rules of fuzzy logic were used. Fuzzy logic is a procedure of numerous valued logic in which the truth values of variables can be any real number among 0 and 1. It is working to control the insight of partial truth where the truth value may range between completely true and completely false which strongly contrasts with the Boolean logic as the truth values of variables may only be the integer values 0 or 1. Fuzzy logic gives the researchers more freedom to work with in comparison to the orthodox methods.

The fuzzy logic is has been utilized be developing the membership function based on fuzzy set of rules. The block diagram for fuzzy set of rules has been presented in Fig. 3.4(a). Initially the fuzzy based system looks for the amplitude range setup against the desired field (DF). After selecting the desired amplitude, the system selects the frequency to pin point the DF. After both amplitude and frequency adjustment, the fuzzy system adjusts the duty cycle according to the sensor's data.

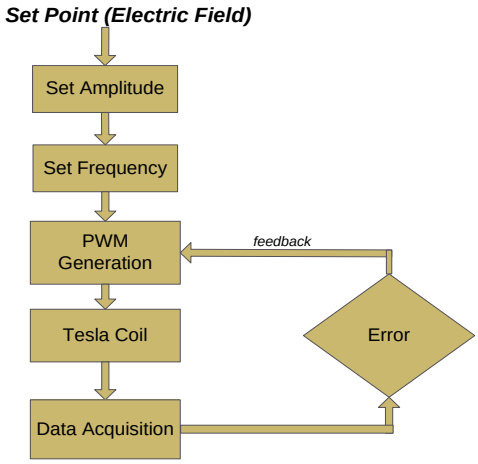

Fig 3.3 (a)

The fuzzy logic is implemented using the method of linear interpolation. The linear interpolation is a mathematical practise of curve fitting which makes use of the linear polynomials to generate different data points within the range of a distinct set of known data points. Linear interpolation is often used to estimate a value of a function using two known values of that function at other points.

We have used the linear interpolation to find the following fuzzy rule state equation:

$$D = 69.93 * FBG - 76.22 * SO$$

Where FBG is feedback gain and SO is system offset and D is duty cycle. Amplitude and frequency are kept constant, whereas the constant values for FBK and SO are experimentally calculated and are verified over the prescribed range. Our system required an Electric Field ranging from 1.2 to 2.4 Tesla. A Change in the Desired Field (DF) causes our system to automatically adjust the duty cycle of PWM and through that the current as well as the required feedback is calculated resulting in the achievement of the desired field at the output.

Later on PWM (Pulse width modulation) technique we used is replaced with PFM (pulse frequency modulation) by incorporating High Frequency Oscillator (HFO) circuit to achieve high level accuracy for generating of electric field of desired field. By the use of High frequency oscillator we can generate the electric fields from 2T to 5T with great accuracy and precision. Fuzzy logic block diagram is show in figure 3.4 (b). First of all the amplitude is set which is 5 in our case. Secondly 50 duty cycles is adjusted then frequency is auto adjusted with the help of HFO and lab view programing logic. Finally this signal is send to tesla coil to generate the desired electric filed. The sensor provide the feedback and data is analysed if the feedback signal does not match with the desired field then system tries to match the difference by adjusting the generated field.

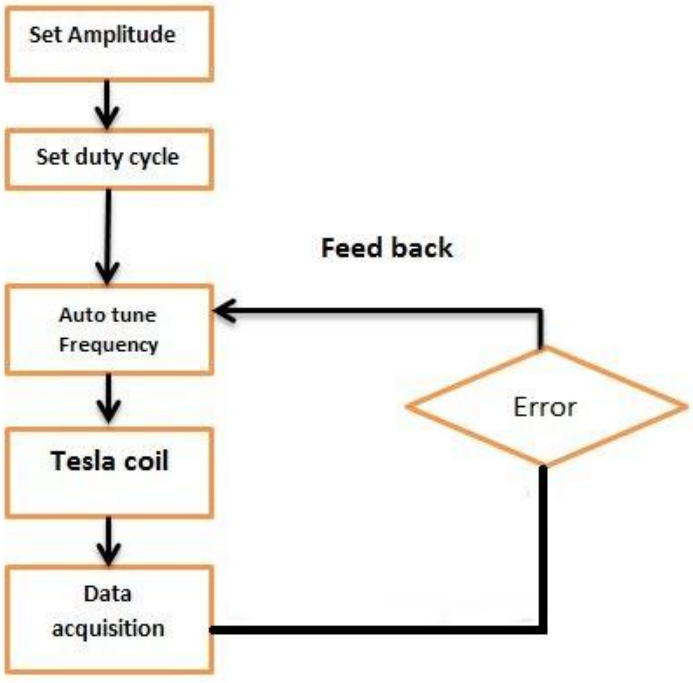

Fig 3.3(b)

3.3.2. A software flow diagram of the system.

The data is acquired using the LABVIEW software. The data will then be configured. Signal conditioning will be used to process the information after it has been properly configured. The signal conditioning is the remodelling of a signal in such a way that sets it up for the approaching phase of processing. Several applications require approximation for example temperature and vibration, from sensors. These signals thus require signal conditioning before a data procurement instrument can viably and precisely measure the signal. Signal conditioning necessitates sampling averaging and filtering of the data. Sampling is the diminishment of a nonstop time data signal to a discrete time data signal. Signal averaging is a signal manipulation process connected in the time space, planned to expand the quality of a signal with respect to noise that is clouding it. By averaging an arrangement of recreated estimations, the signal to-noise ratio, S/N, will be enhanced, preferably in extent to the square base of the quantity of estimations. A filter is an instrument or a process that minimizes certain undesirable aspects or components from a signal. Filtering is a category of signal processing, the characterizing highlight of filters being the fact that they are capable of removing entire or fractional part of the signal. Frequently, this implies evacuating a few frequencies or frequency groups.

Bias, alignment and sensitivity errors are impacts that strike with fluctuating degrees in all sensors, particularly inertial sensors, and they impact the precision of the signals delivered by those sensors. To overcome these variations, calibration strategies will be applied to the data signal.

At this point the data signal will be integrated with the hardware. Finally the electric field will be adjusted through a data acquisition feedback between the hardware and the software of the system. Data acquision (DAQ) is the technique towards approximating an electrical or physical phenomenon for example voltage, current, temperature, weight, or sound with a computer. A DAQ frame work includes of sensors, DAQ estimation equipment, and a PC with programmable programming. At the point when contrasted with the universal estimation frameworks, advanced DAQ frameworks productively use the making power, productivity, show, and network abilities of industry standard PCs giving an all the more capable, , practical and an adaptable approximation procedure.

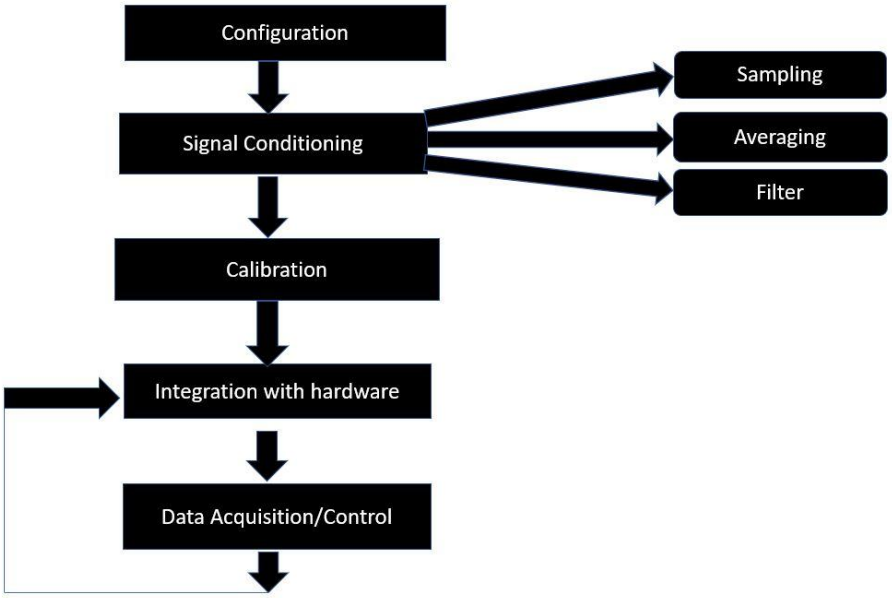

Fig 3.4 : A software flow diagram of the system

3.4. System Architecture

Our system has utilized National Instruments (NI) DAQ USB 6001 as the main controller. NI DAQ USB 6001 had an input range of ±10 V. It has an inbuilt counter. It has 8 analogue inputs, 2 analogue outputs, and 13 digital input output pins.NI DAQ card is connected with tesla coil and sensor module. Hall Effect sensor module was attached to the DAQ card to sense the generated electric field. The range of this sensor is 30 A. The repeatability of the sensor used is 3 mA. Tesla coil was used for the electric field generation. PWM signal is generated by lab view software and given to tesla coil. Later on this PWM signal is replaced with PFM signals by incorporating High frequency oscillator circuit designed. Designed HFO generates oscillating frequencies up to 15MHz.

An input is given to the DAQ card through NI Lab View. Tesla coil generates the field given as the input. Feedback sensor senses the electric field generated by the tesla coil. In case of an error a feedback is given to the controller by the feedback sensor, which corrects the error and hence the system operates.

3.4.1. System constraints

A lot of trial and error was involved in the process. Several compromises were made to achieve a trade-off between the cost and the performance. Initially a high end DAQ was to be used as it was thought to be available, later on it became unavailable so we had to buy it ourselves. We bought a low-cost multifunction DAQ USB 6001 as it was affordable. With this downgrade we had to change our software design because we had to design PWM simulation on the LabView software as this card did not have the

in-built ports to work with pulse width modulated signals. So, our software program had to be modified accordingly to accommodate for that.

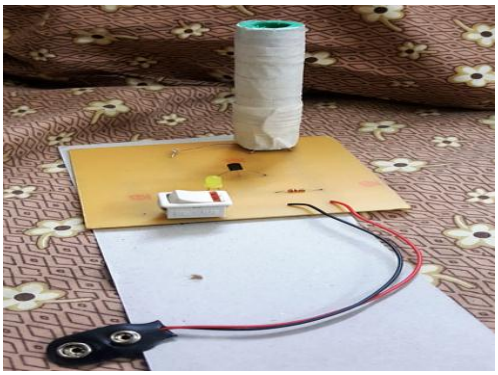

Fig 3.5. shows the simple tesla coil implemented on PCB

Initially we designed a circuit for tesla coil and implemented it on a PCB. This simple tesla coil is shown in figure 4.2. Later on we realised that for digital use we needed a solid-state tesla coil. So, we designed a SSD tesla coil which was compatible with the digital software.

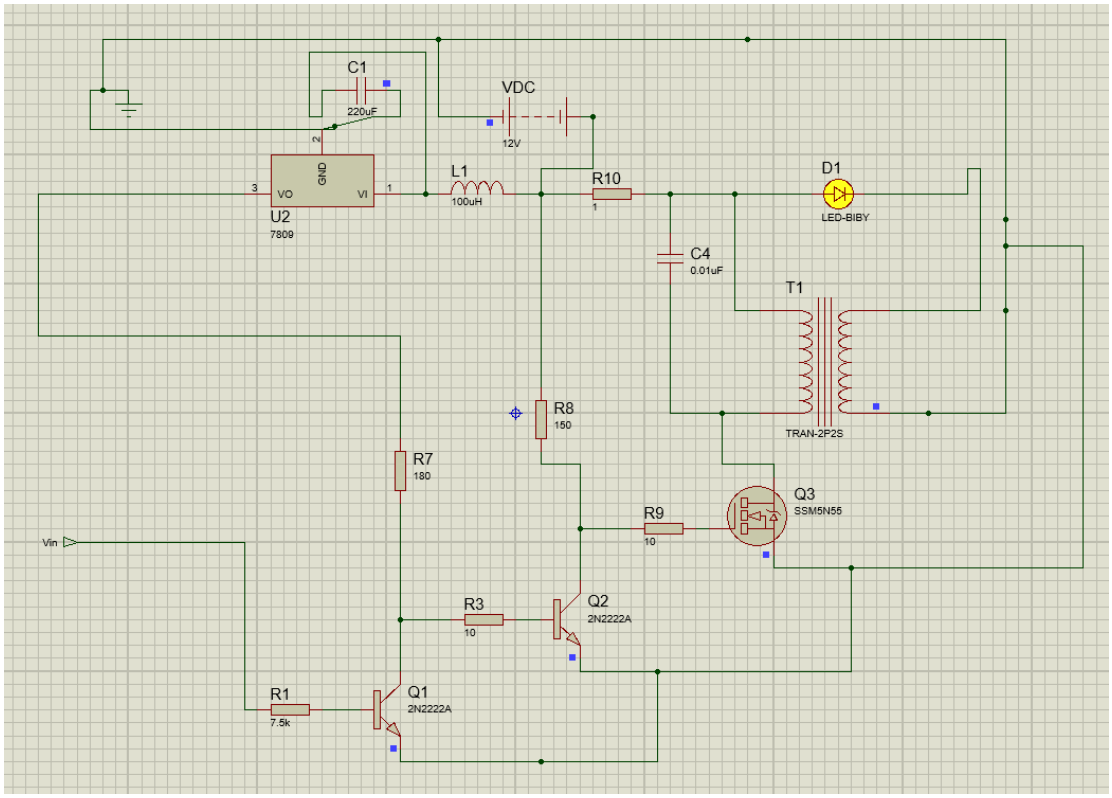

Fig 3.6 shows the Porteous simulation of the modified SSD tesla coil

Initially we tried to use SSD tesla coil whose pulsing was based upon 555 timer IC and related components. Later on, we designed its logic on the software for it be controlled through the software. Figure 4.0 shows the Porteous simulation of the modified SSD tesla coil. This not only reduced the hardware of the system but also in turn minimized the hardware cost as well.

3.4.2. Hall Effect Sensor.

We used a Hall Effect sensor IC module of range 200A. This sensor is shown in the fig 3.8.To calibrate it we took samples on a very small range due to which sensor results were not as accurate compared to the datasheet. We could not test it at such

high currents because we could not find a current source that would be able to generate current as high as that. The non-availability of high current source forced us to use a sensor of range 30 A.

Fig 3.7: A 200 A Hall Effect Sensor Module

Hall Effect sensor Module: ACS 712x30A modules are used for measurement of the generated electric field. The range of this sensor is 30 A. The repeatability of the sensor used is 3 mA.

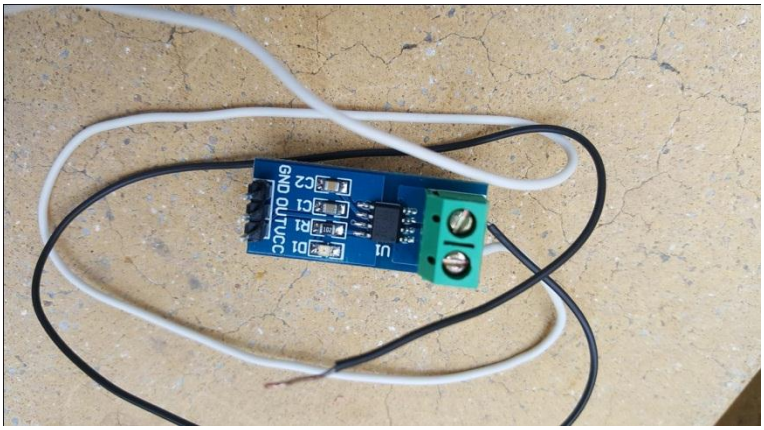

Fig 3.8: showing the ACS 712x30A module acquired

3.4.3. Sensor Calibration

We calibrated the Hall Effect sensor by giving different samples of currents on input terminals provided by DC power supply. First of all we found out the offset voltage of the Hall Effect sensor module and then we found out the voltages corresponding to the respective current inputs. The following results were obtained.

Input Current (I) in Amperes	Output Voltage (V) in volts
0.0	2.54
0.5	2.57
1.0	2.60
1.5	2.63
2.0	2.67
2.5	2.70
3.0	2.73
3.5	2.76
4.0	2.80
4.5	2.83
5.0	2.86

Table 3.1: displays the readings obtained for the sensor calibrations

Calculations performed regarding the calibration of the sensor are stated below.

$$m = \frac{y_2 - y_2}{x_2 - x_1}$$

$$m = \frac{2.86 - 2.54}{5 - 0}$$

$$m = \frac{0.32}{5}$$

$$m = 0.06$$

3.4.4. Mathematical calculations.

$$v = mI + v_o$$

$$I = \frac{v - v_o}{m}$$

$$I = \frac{2.63 - 2.54}{0.06}$$

$$\boldsymbol{I = 1.5\ A}$$

3.5. System Implementation

We gave input to Tesla coil through DAQ card using the LabView software. For example 5 tesla input is given to the DAQ card through LabView. Suppose at that moment the given input of 5 tesla is not being generated by the SSD tesla coil. Hall Effect Sensor module then measures the field and gives feedback to the USB DAQ which in turn enables LabView to accordingly vary the width of PWM. A control of the electric field generation had been achieved using this method.

3.5.1. Tools and Technology Used.

Stated below are the details of hardware tools and the software technologies used to get the system functioning.

Hardware part of the system comprises of:

3.5.2. National Instruments (NI) DAQ Card USB 6001:

The USB6001 is a nominal cost, multi-function DAQ gadget. It deals analogue simple I/O, digital I/O, and a 32 bit counter. The USB6001 provides fundamental utility to applications for example basic information logging, versatile estimations, and scholastic lab tests. The device comprises of a light weight transport controlled mechanical enclosure for simple compactness. The sensors and signals can be easily connected to USB 6001 using a screw-terminal network. The input range of the card is ±10 V. It has an inbuilt counter. It has 8 analog inputs, 2 analog outputs, and 13 digital input output pins.

Fig 3.9: showing NI DAQ USB 6001 that we shipped from the US

3.5.3. Solid-State Tesla Coil:

The solid state tesla coil is made up of a 75000 ohms resistor, a 5000 ohms resistor, a 10 ohms resistor, a 150 ohms resistor, a 180 ohms resistor, two 2N222A transistors, a 100 mF inductor, a 0.01 µF capacitor, a 220 µF capacitor, an FET transistor, LM 7809 +9 voltage regulator and a fly back transformer.

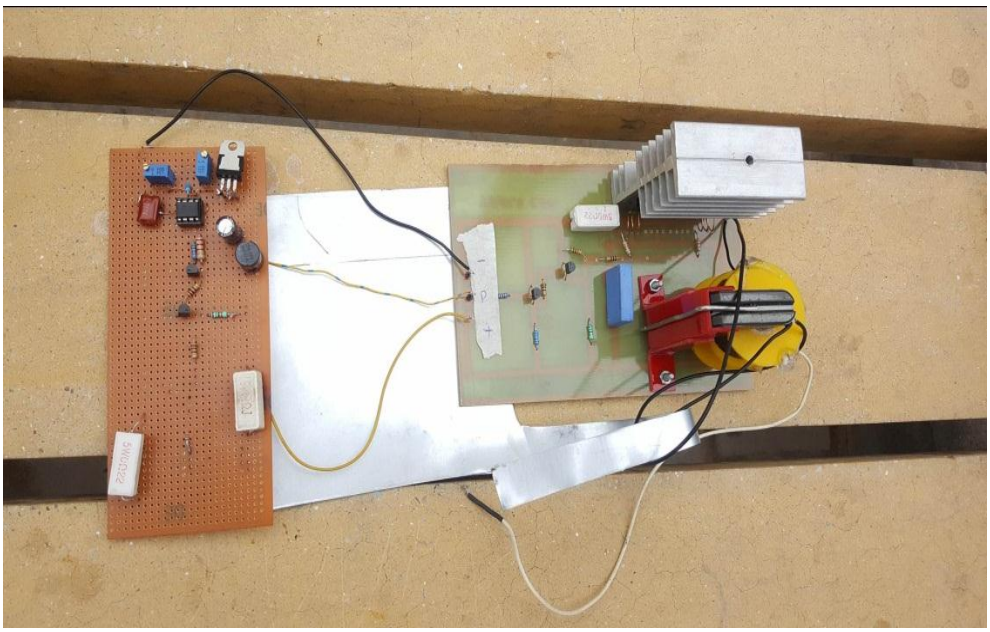

Fig 3.10: showing the designed SSD Tesla Coil

3.5.4. Hall Effect sensor Module:

ACS 712x30A module is used for the measurement of the generated electric field. The range of this sensor is 30 A. The repeatability of the sensor used is within 3 mA.

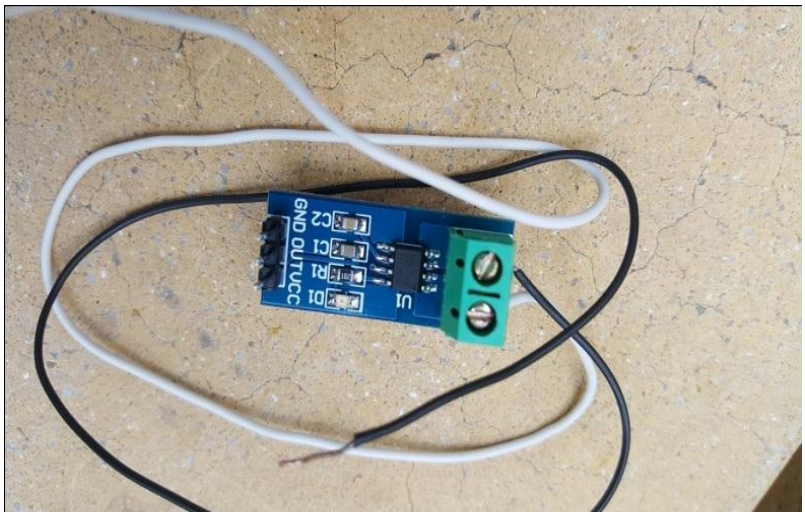

Fig 3.11: showing the ACS 712x30A module acquired

Software part of the system includes:

- NI Lab VIEW 2014: Lab VIEW is charters developing programming for applications that require testing, approximation, and control with fast access to apparatus and information bits of information.
- NI-DAQ mx 17.0: NI-DAQmx driver programming goes a long way past a fundamental DAQ driver to convey expanded efficiency and execution and is one of the principle reasons National Instruments keeps on being the pioneer in virtual instrumentation and PC-based information procurement.

3.5.5. Sensor Calibration Processing Logic/Algorithm.

Fig 3.13 shows the logic used to calibrate the sensor. The Lab VIEW logic diagram demonstrates the input, output modules as well as the off-set blocks for the calibrations of the Hall Effect sensor module. The figure portrays the logic used to calibrate the sensor. Voltage inputs were given to the DAQ card using the Lab VIEW software. The Hall Effect sensor module's outputs were obtained corresponding to the input voltage values.

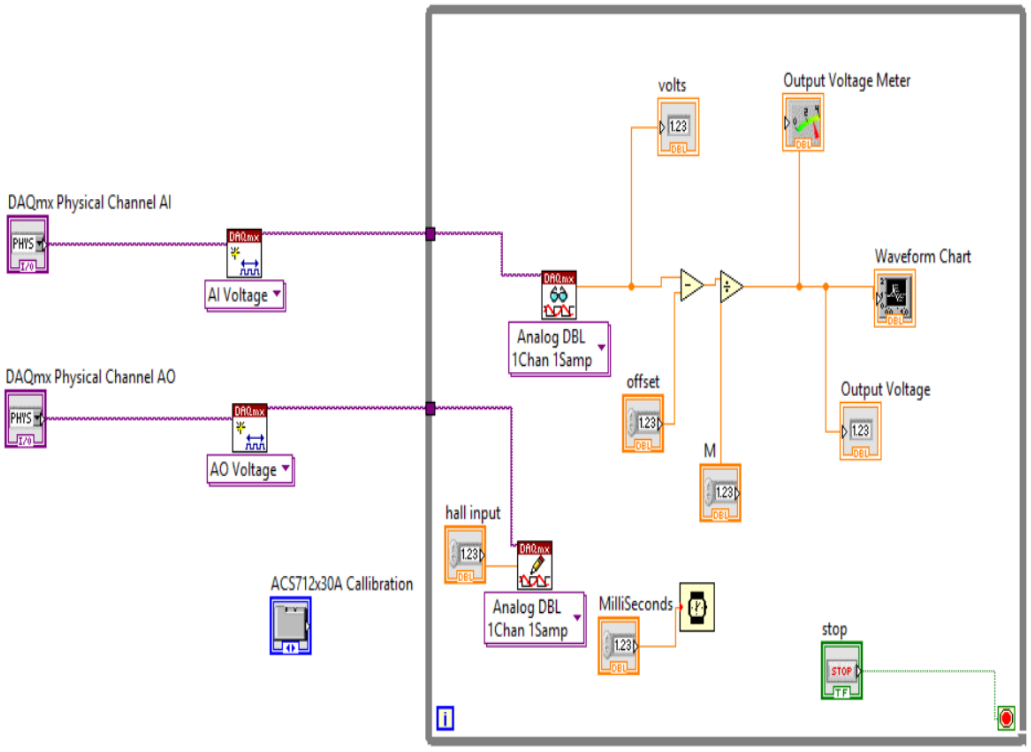

Fig 3.12 shows the logic implementation for the sensor calibration

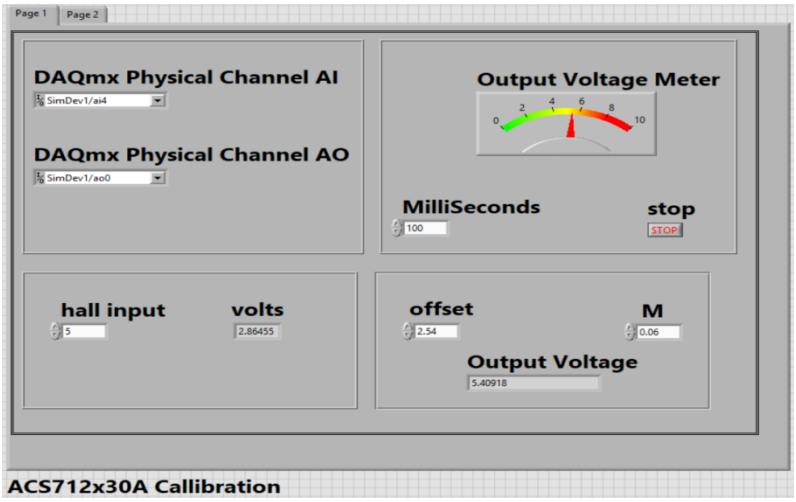

Fig 3.13 shows the front panel for the sensor calibration in LabVIEW

The front panel of the Lab VIEW software has been shown in the duration of the sensor calibration. Hall input is given to the DAQ card through this software. The inputs are given to the DAQ mx Physical Channel Analog input and outputs are obtained from DAQ mx Physical Channel Analog output.

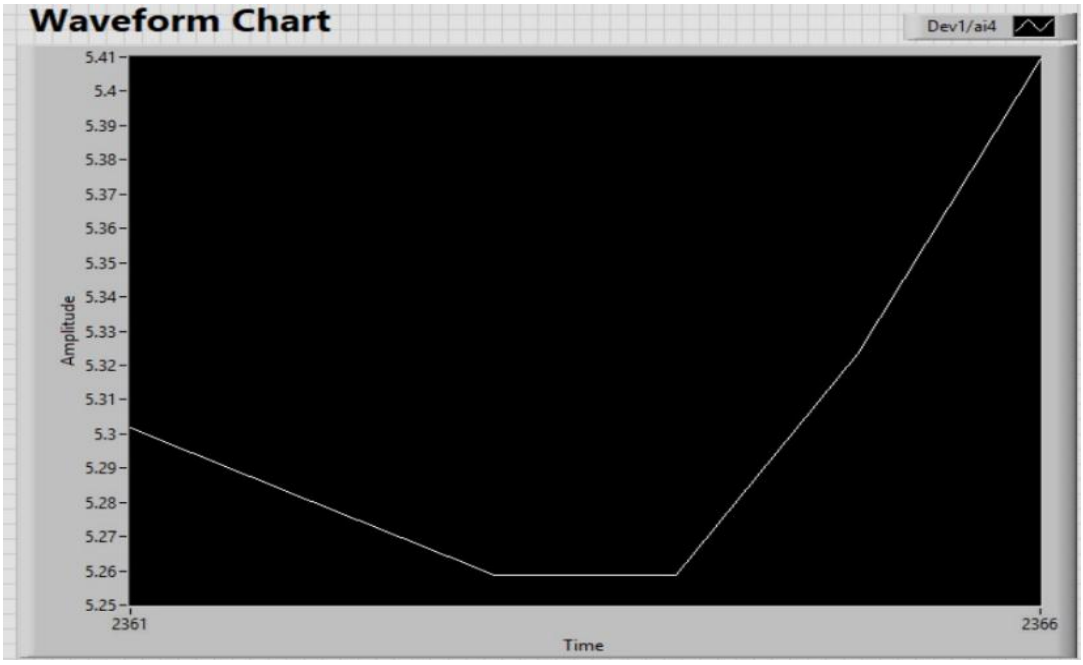

Fig 3.14.shows the graph obtained during the sensor calibration

3.6. High Frequency Oscillator (HFO) Design:

The PWM technique was later modified to PFM (pulse frequency modulation). This modification is carried away by designing high frequency oscillator circuit of frequency 20 MHz's The HFO generates signals of variable frequency which is given to the tesla coil input as pulse. Due to incorporation of HFO the accuracy of the system is enhanced and electric fields of 2T to 5T can be generated accurately. The circuit simulation and design is shown in figure.

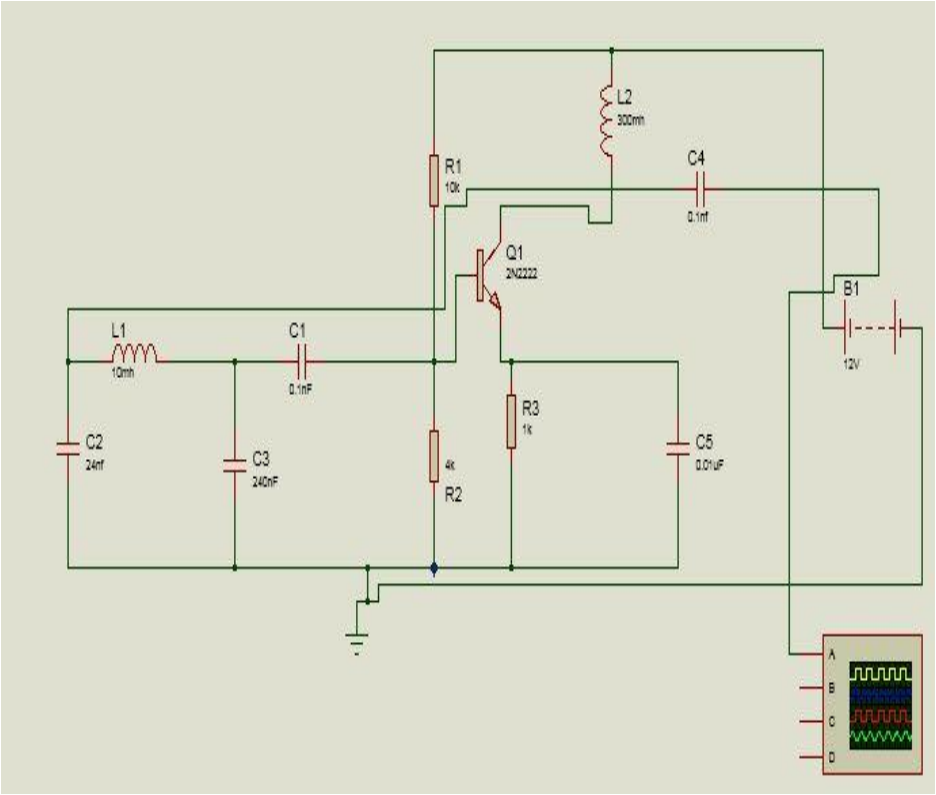

Fig 3.15 : High Frequency Oscillator circuit simulation.

3.7. Block Diagram (Lab View) of Programming logic for PWM.

The Fig 3.16 shows the programing logic designed in lab view. Analog channels are created because of input to the controller is analog signals. DAQ assistance module provides the connectivity with the controller. After acquiring the signals from the sensor these signals are displayed as graphs. In PWM technique duty cycle changes according to the systems input, frequency and amplitude parameters are constant. Gain (K), feedback gain (FBG) and Feedback offset (FO) are the tuning parameters of the system.

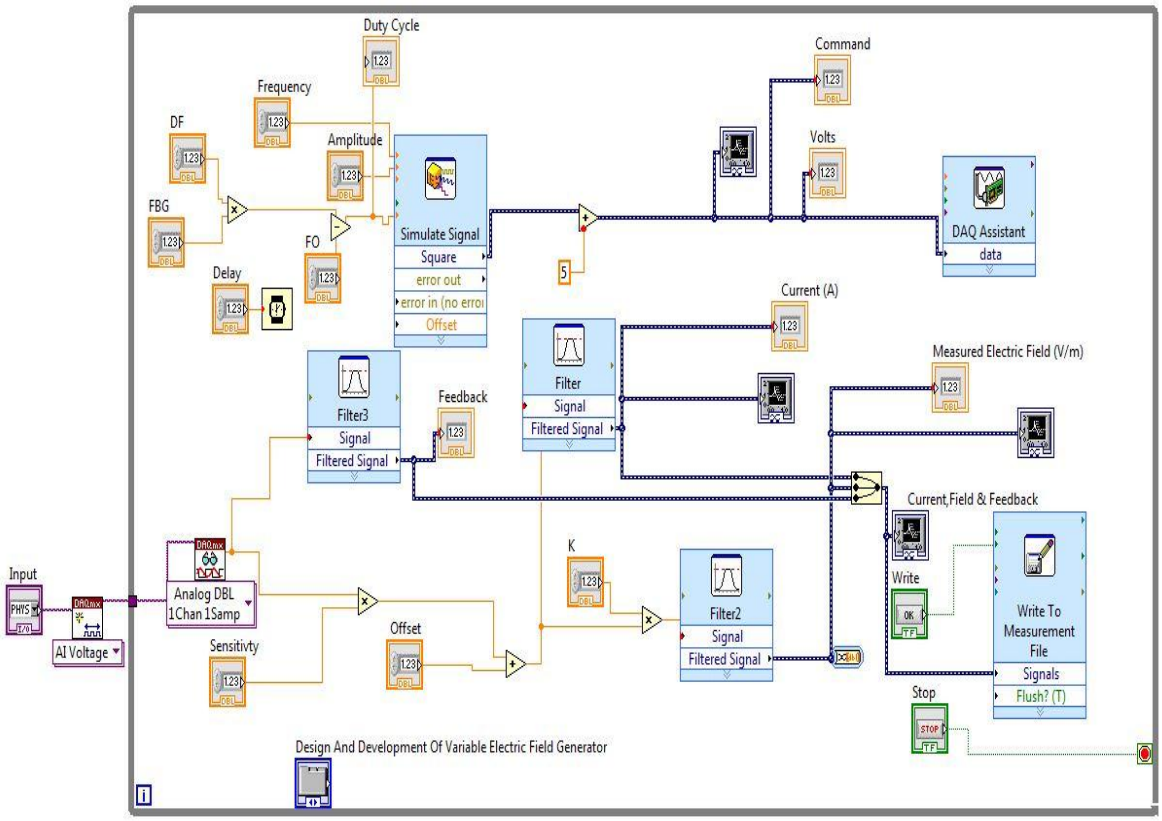

Figure 3.16: system programming for PWM.

3.8. Block Diagram (Lab View) of Programming logic for PFM.

Fig 3.17 shows the block diagram of programing logic created in lab view for PFM technique incorporated using HFO. In this logic the duty cycle and amplitude are fixed while frequency is being varied to generate the higher electric field that PWM technique was not able to produce. By using this technique system generates the electric fields of 2T to 5T effectively.

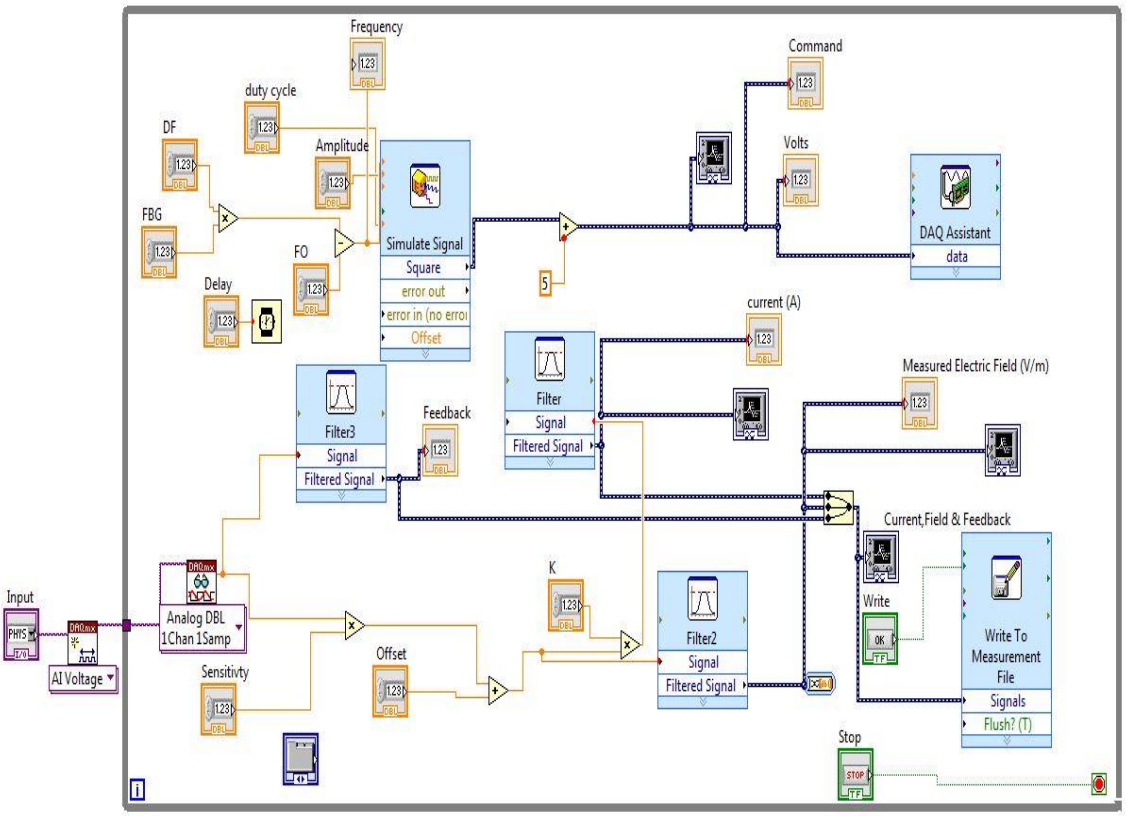

Figure 3.17: System programming logic for PFM

Chapter 4

Evaluation

CHAPTER 4. EVALUATION

4.1. System Setup

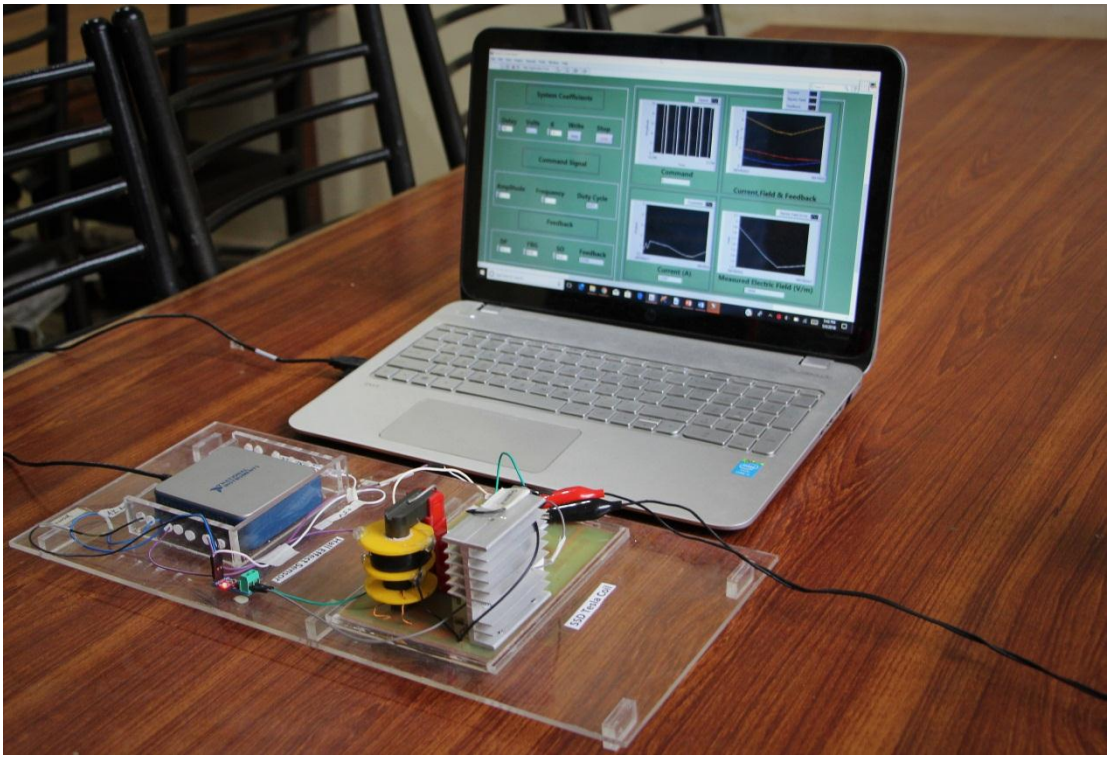

Fig 4.1: Shows the complete system setup

4.2. System Evaluation and Results based on PWM.

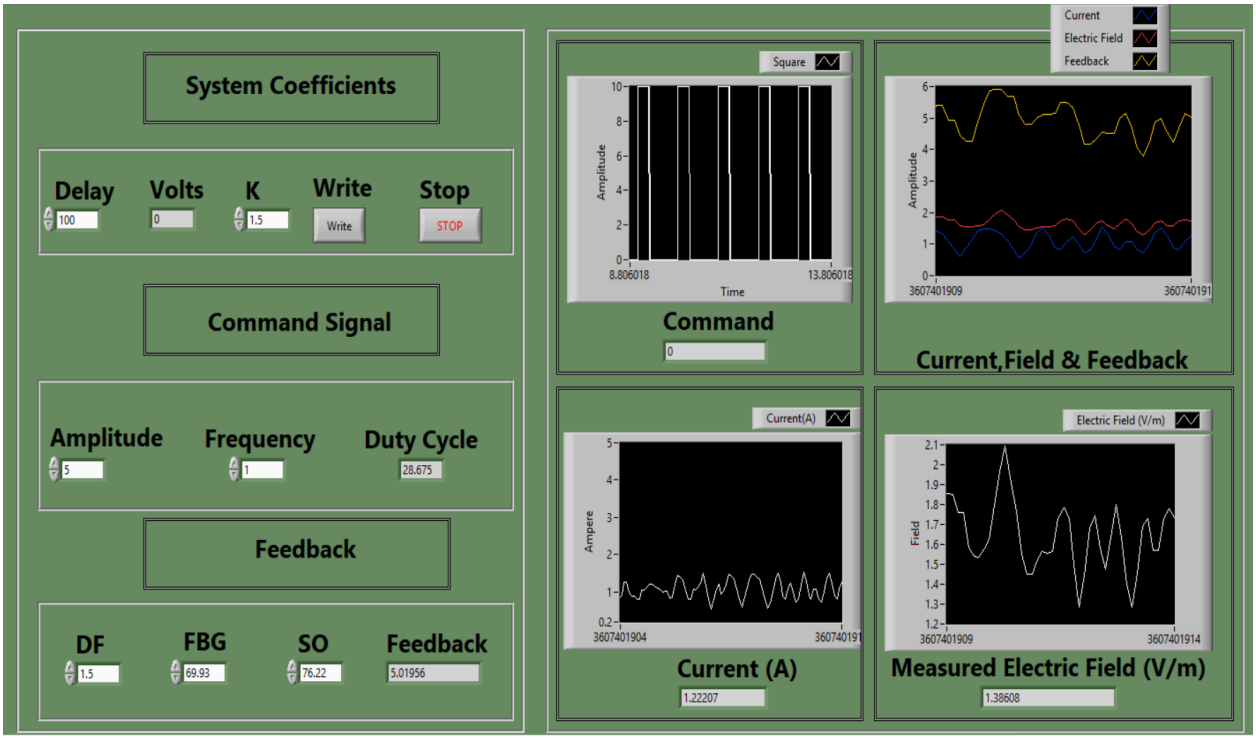

Fig 4.2: Complete flow of the system (PWM)

The front panel of the Lab VIEW software has been displayed in Fig 4.2. The first tab shows the values assigned to the system coefficients. The second tab shows the command signal where different variables are given. The feedback blocks presents the input which is the Desired Field (DF), along with the feedback gain (FBG), system offset (SO) and the feedback. The inputs are given to the DAQ mx Physical Channel's Analog input and outputs are obtained from DAQ mx Physical Channel's Analog output. The input and output graphs are displayed next to the tabs in the VI. There are

four graphs each displaying a distinct set of information. The top graphs represent the system input. The top left graph shows the command/input while the top right graph displays all the parameters on the same chart. The bottom graphs depict the system output. The bottom left graph displays the output current while the bottom right graph displays the Electric Field generated as a result of the given input.

Our fuzzy based system operated on the variation of a single parameter. The DF is applied as an input. The duty cycle of the PWM changes in response to the applied input using the previously discussed fuzzy rules. Hence using the feedback mechanism, the desired field is achieved. The other factors including FBG, SO and K were all kept constant throughout and are calculated experimentally.

The results for an input ranging from 1.2T to 2.4T have been tested in 6 alterations as follows.

4.2.1. 1ST Alteration:

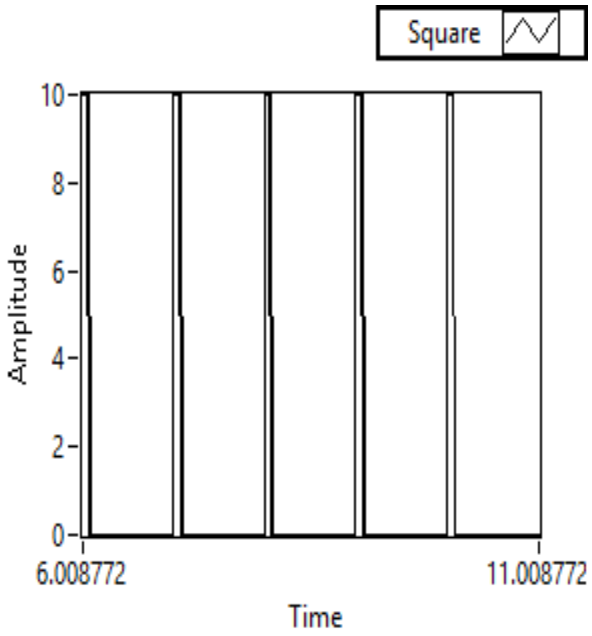

Fig 4.3 : PWM Command Graph for the 1st alteration.

At first the 1st alteration/desired field of 1.2T was provided to the system. Fig. 4.3 shows the graph of required PWM to achieve desired field. Fig. 4.4 displays a graph obtained of the feedback, current and electric field generated against the desired field. The graph illustrates that the measured/output field came out to be 1.2539T when the input of 1.2T was given to the system. Moreover, the plot presents the ratio of current in terms of electric field.

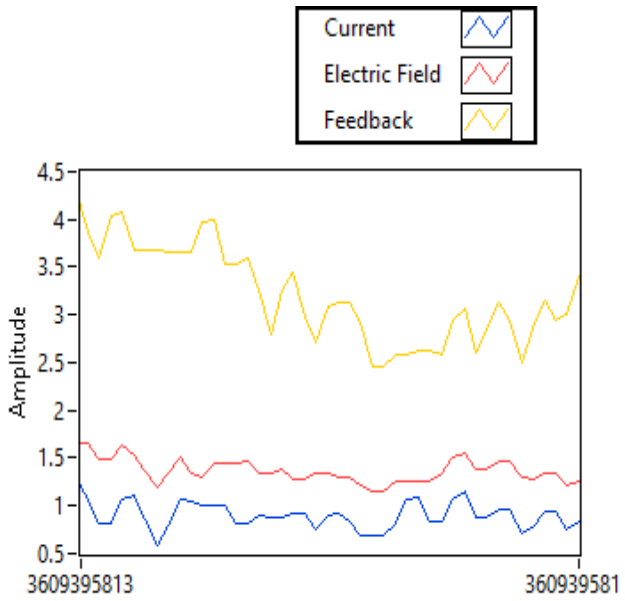

Fig 4.4: A graph of the feedback, current and electric field generated for 1st alteration.

4.2.2. 2ND Alteration:

Following that a 2nd alteration/desired field of 1.5T was provided to the system. Fig. 4.5 shows the graph of the PWM generated in response to the 2nd input. Fig. 4.6 displays a graph obtained of the feedback, current and electric field generated against the desired field. Current generated at the tesla coil's output is shown in the graph in

relationship with the generated field. The graph illustrates that the measured/output field came out to be 1.54955T when the input of 1.5T was given to the system.

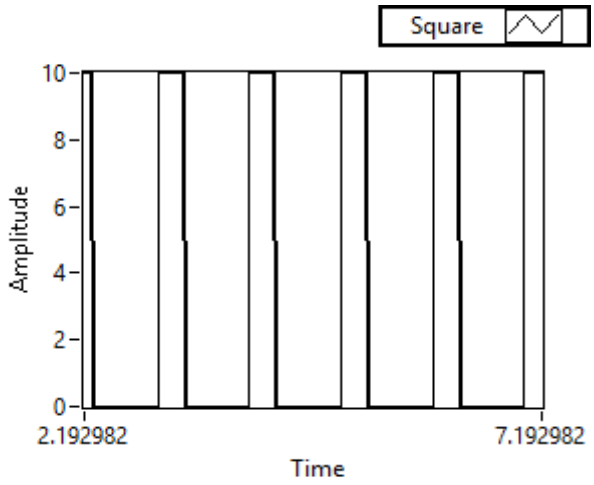

Fig 4.5: PWM Command Graph for the 2nd alteration.

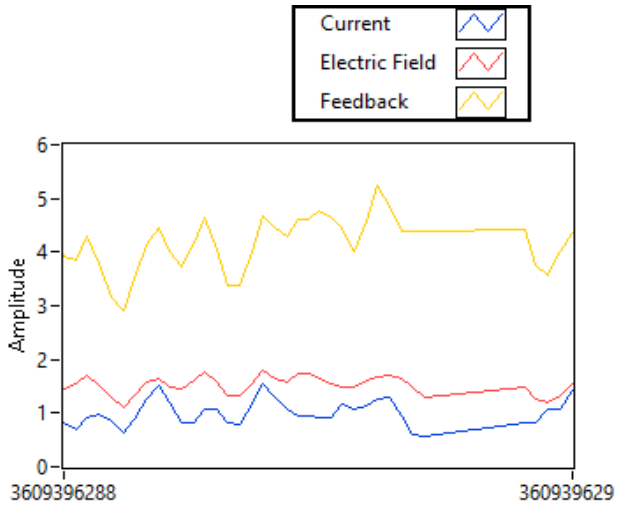

Fig 4.6: A graph of the feedback, current and electric field generated against the 2nd alteration.

4.2.3. 3RD Alteration:

3rd alteration / desired field of 1.8T was provided to the system. Fig. 4.7 shows the graph of the PWM needed to achieve the required D.F for the 3rd input. Fig. 4.8 displays a graph obtained of the feedback, current and electric field generated against

the desired field. The current generated at the conjunction with the field shows the ruggedness of the algorithm. The graph also illustrates that the measured/output field came out to be 1.86768T when the input of 1.8T was given to the system.

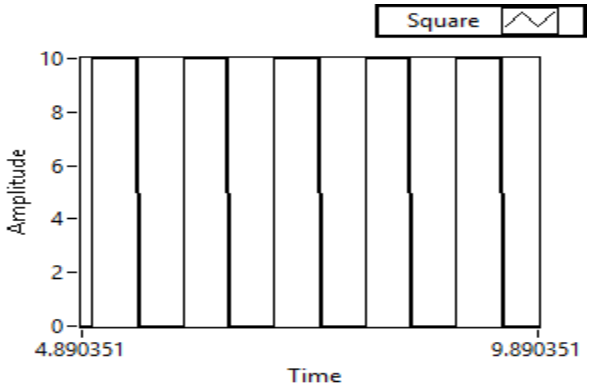

Fig 4.7 : PWM Command Graph for the 3rd alteration.

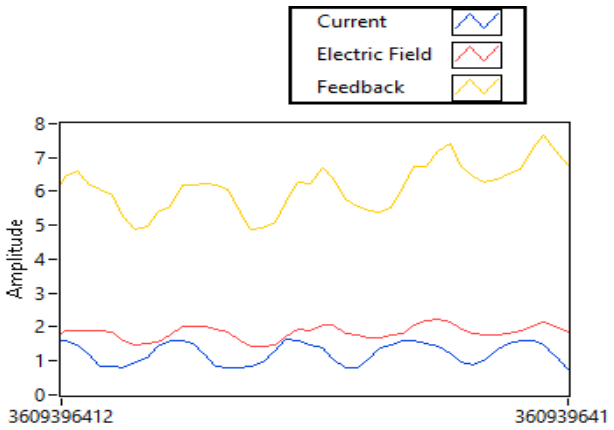

Fig 4.8: Feedback, Current and Electric field generated for 3rd alteration.

4.2.4. 4TH Alteration:

Following that a 4th alteration/desired field of 2.0T was given to the system. Fig. 4.9 shows the graph of the PWM generated in response to the 4th input. Fig. 4.10 displays a graph obtained of the feedback, current and electric field generated against the

desired field. The graph depicts the current generated across the tesla coil as well as the measured / output field. The obtained field came out to be 2.01955T when the input of 2.0T was provided to the system.

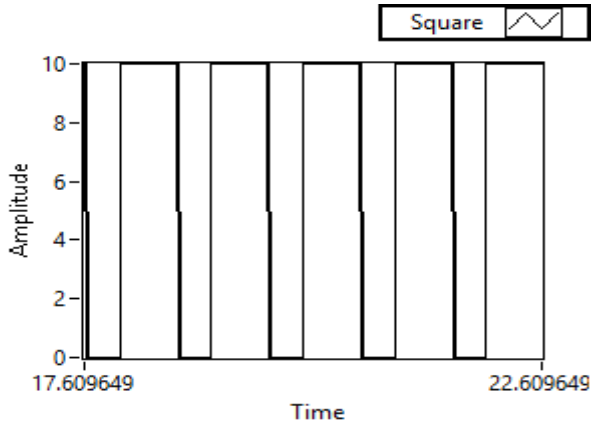

Fig 4.9 : PWM Command Graph for the 4th alteration.

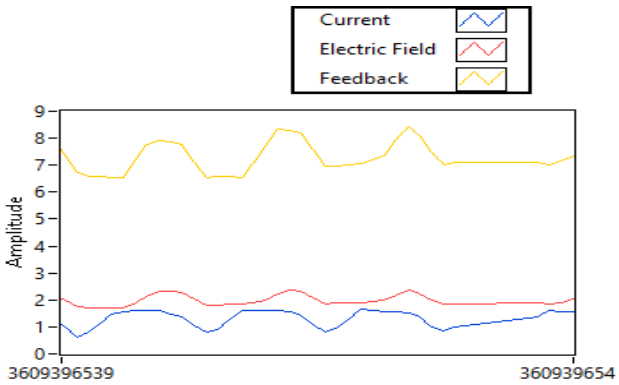

Fig 4.10: Feedback, Current and Electric field generated for 4th alteration.

4.2.5. 5TH Alteration:

After that the 5th alteration/desired field of 2.2T was provided to the system. Fig. 4.11 shows the graph of the PWM needed to achieve the required D.F for the 5th input. Fig. 4.12 displays a graph obtained of the feedback, current and electric field generated

against the desired field. The graph in Fig.4.12 illustrates that the measured/output field came out to be 2.27532T when the input of 2.2T was given to the system.

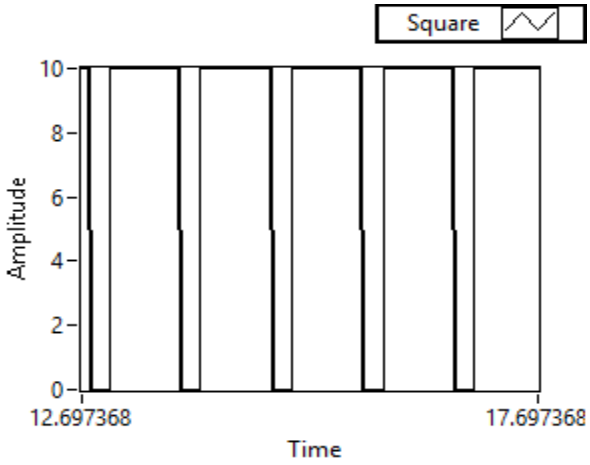

Fig 4.11 : PWM Command Graph for the 5th alteration.

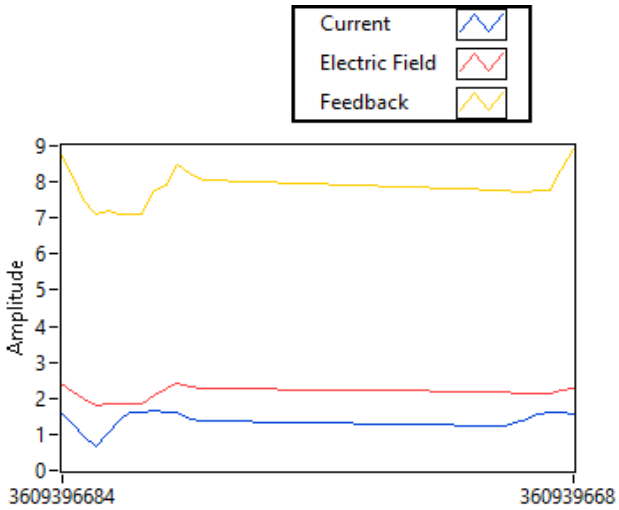

Fig 4.12: Feedback, Current and Electric field generated for 5th alteration.

4.2.6. 6TH Alteration:

Finally, a 6th alteration/desired field of 2.4T was given to the system. Fig. 4.13 shows the graph of the PWM generated in response to the 6th input. Fig. 4.14(a) displays a graph obtained of the feedback, current and electric field generated against the desired

field. The graph illustrates that the measured/output field came out to be 2.41128T when the input of 2.4T was provided to the system.

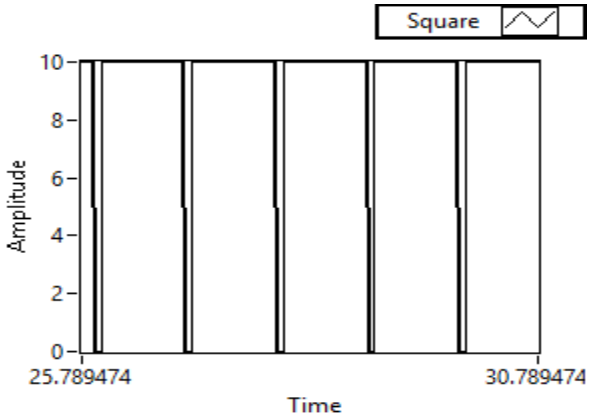

Fig 4.13: PWM Command Graph for the 6th alteration.

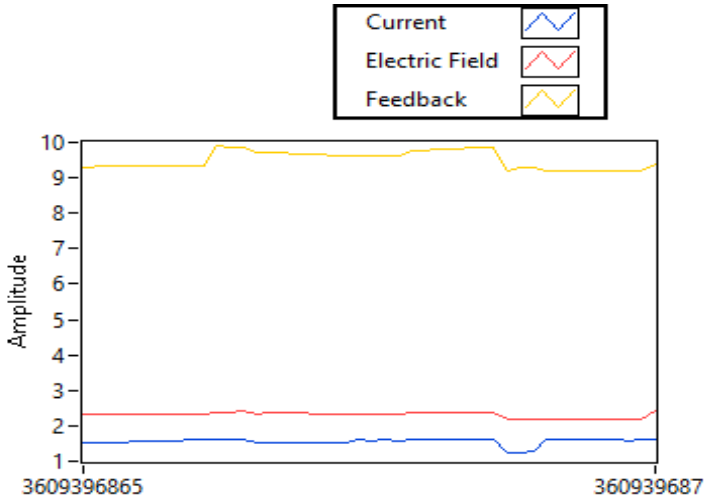

Fig 4.14(a): Feedback, Current and Electric field generated for 6th alteration.

The comparison of electric field generated against the desired field, duty cycle along with error has been presented in Table: 4.1. It can be seen from Table:4.1 that fuzzy membership function has been using 10VDC amplitude and 1.0 Hz frequency to attain the desired field with a maximum percentage error of 0.07532 by adjusting the Duty Cycle of the input signal between 10% to 90%. The desired field has been varied between 1.2T to 2.4T and the results have been tabulated in Table 4.1.

Sr.	Desired Field, DF (Tesla)	Fuzzy based Set of Set of Membership Functions			Measured Field (Tesla)	Error
		1. Amplitude (V)	2. Frequency (KHz)	3. Duty Cycle (%)		
1.	1.2	10	1.0	10	1.2539	0.0593
2.	1.5			25	1.54955	0.04955
3.	1.8			40	1.86768	0.06768
4.	2.0			60	2.01955	0.01955
5.	2.2			80	2.27532	0.07532
6.	2.4			90	2.41128	0.01128

Table. 4.1: Summary of Fuzzy based Membership Functions with Measured Field and Error based on PWM.

Graph 4.14(b) represents the relationship between the desired EF and generated EF by the system.

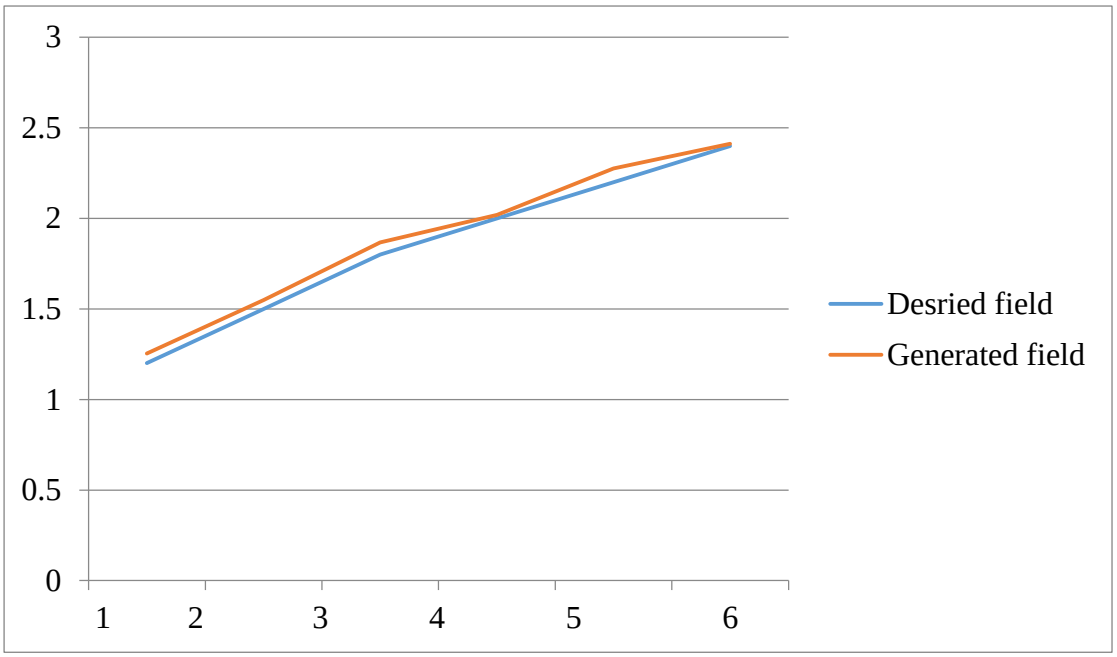

Fig 4.14(b): Graph representing relationship between desired EF and generated EF.

4.3. System Evaluation and Results based on PFM.

4.3.1. 1st Alteration:

The 1st alteration/desired field of 2T were provided to the system. Fig. 4.16 shows the graph of required PFM to achieve desired field. Fig. 4.17 displays a graph obtained of the feedback, current and electric field generated against the desired field. The fig 4.19 graph illustrates that the measured/output field came out to be 2.05674T when the input of 2T was given to the system.

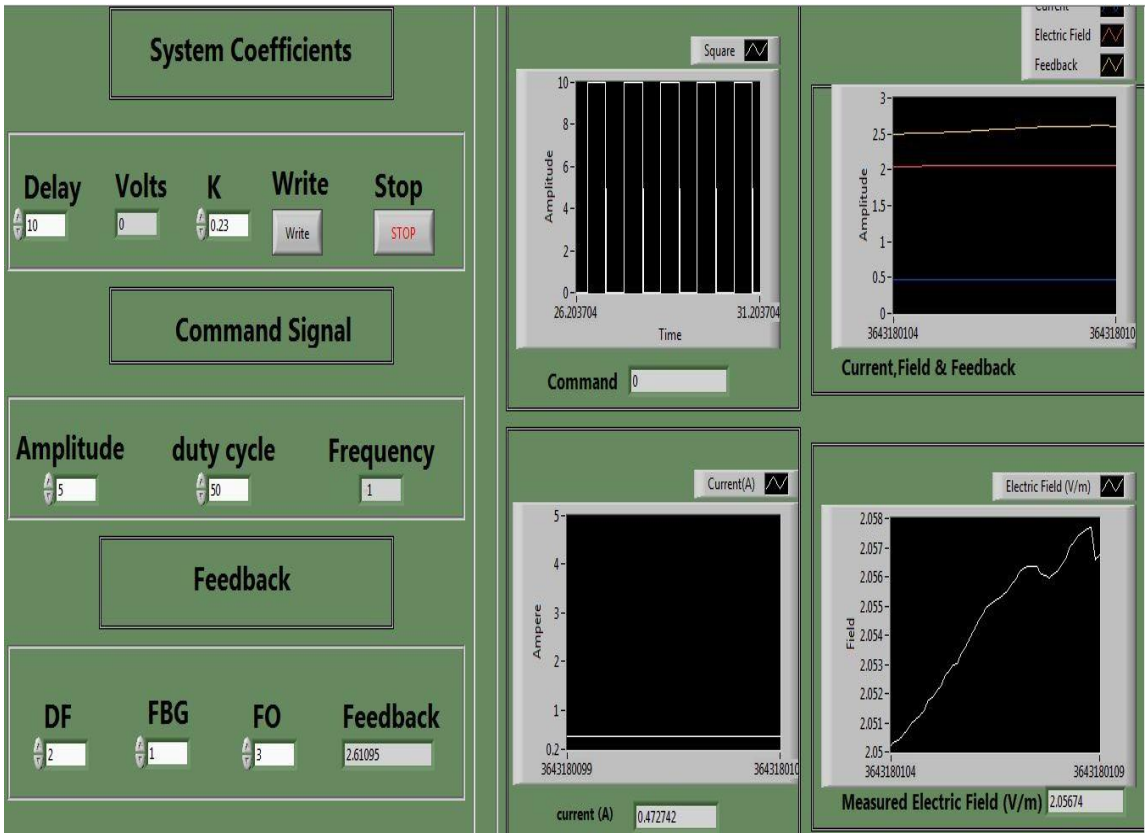

Fig 4.15: Complete system parameters and flow of the system (PFM)

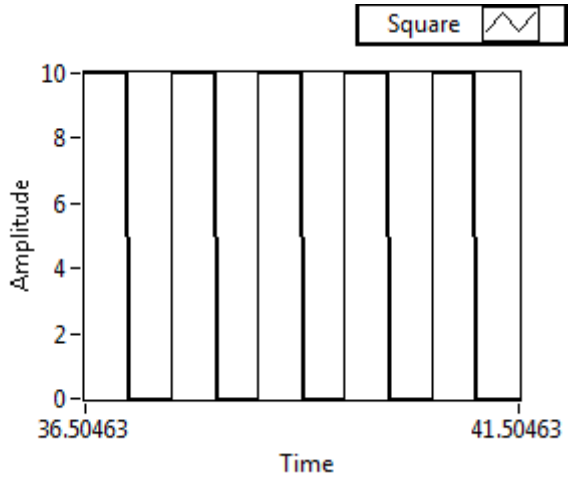

Fig 4.16: PFM Command Graph for the 1st alteration.

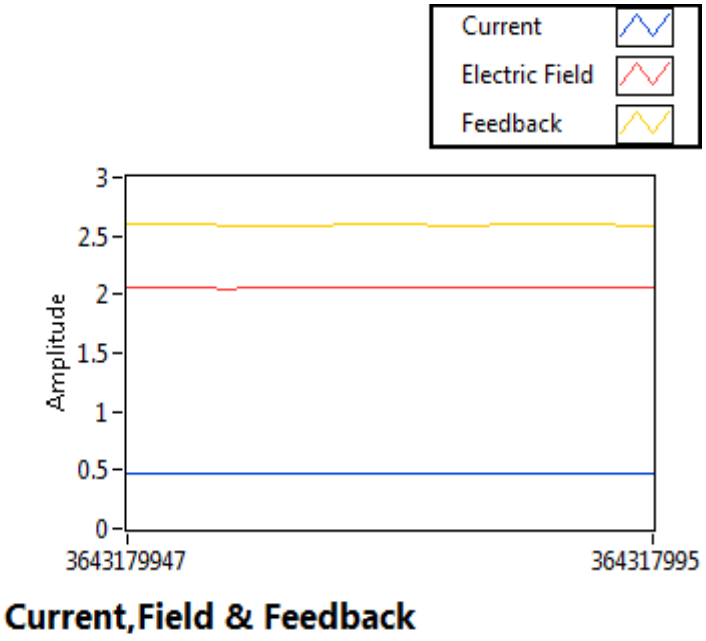

Fig 4.17: Feedback, Current and Electric field generated for 1st alteration.

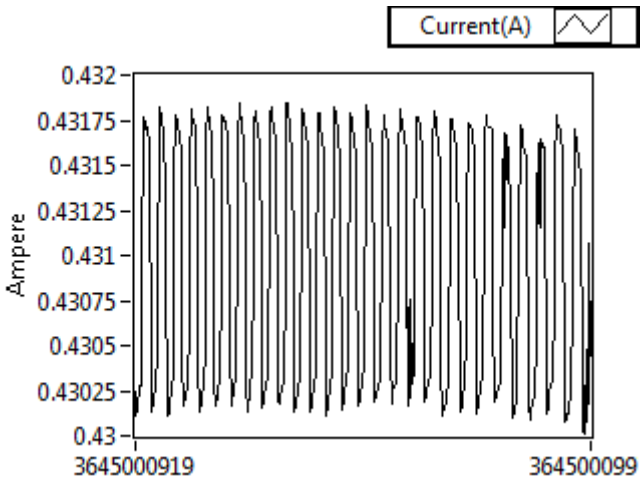

Fig 4.18: Current output for 1st alteration.

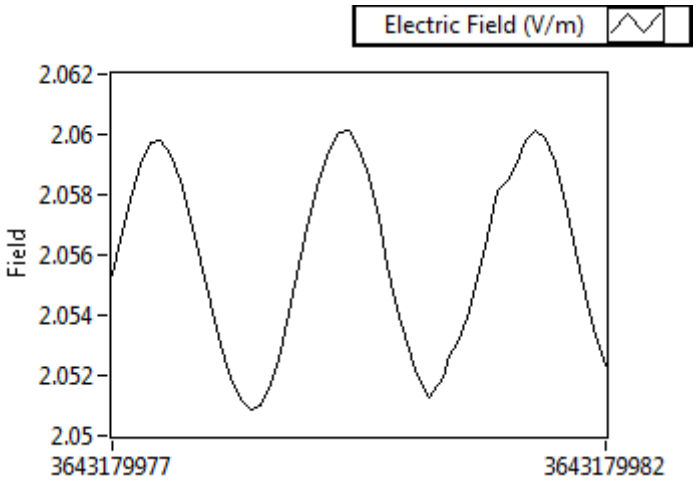

Fig 4.19: Electric field generated for 1st alteration.

4.3.2. 2nd Alteration:

At the 2st alteration/desired field of 2.5T was provided to the system. Fig. 4.21 shows the graph of required PFM to achieve desired field. Fig. 4.22 displays a graph obtained of the feedback, current and electric field generated against the desired field.

The Fig 4.24 graph illustrates that the measured/output field came out to be 2.51094T when the input of 2.5T was given to the system.

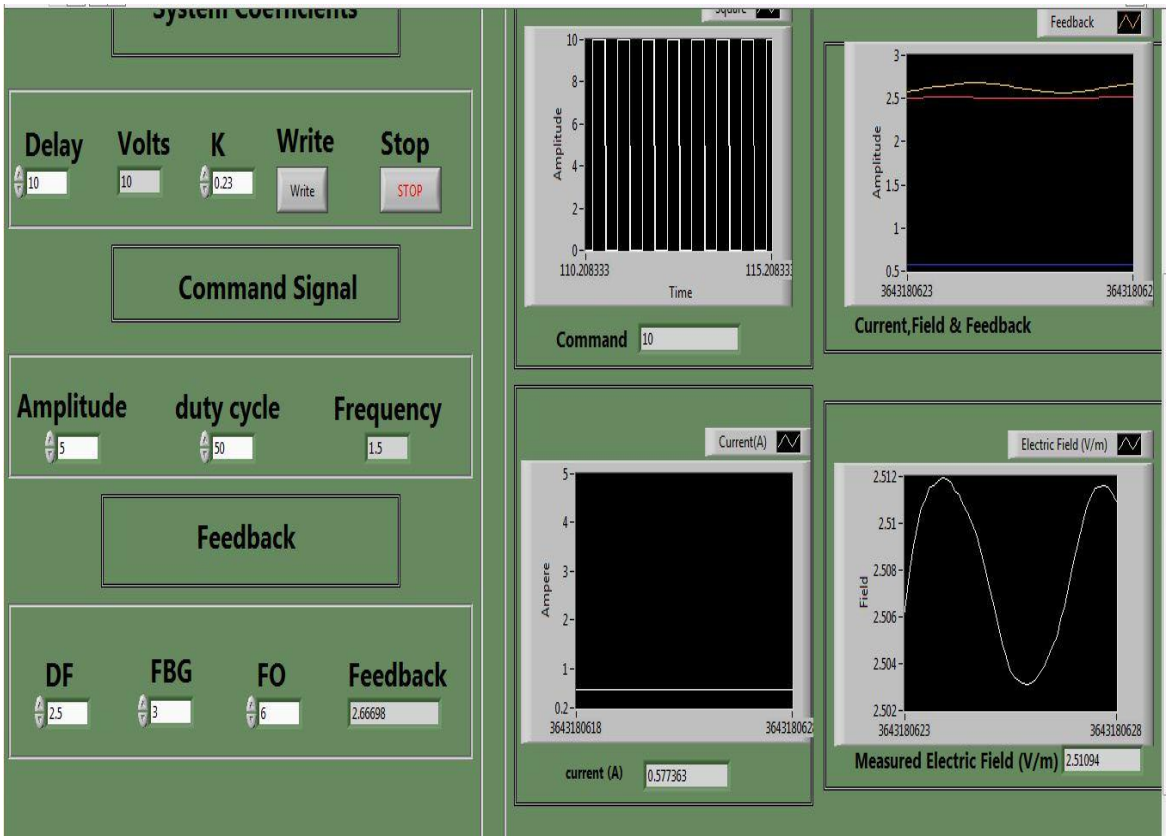

Fig 4.20: Complete system parameters and flow of the system (PFM)

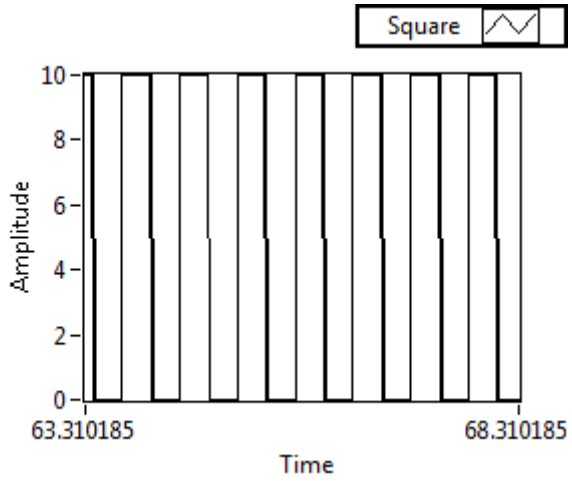

Fig 4.21 : PFM Command Graph for the 2nd alteration.

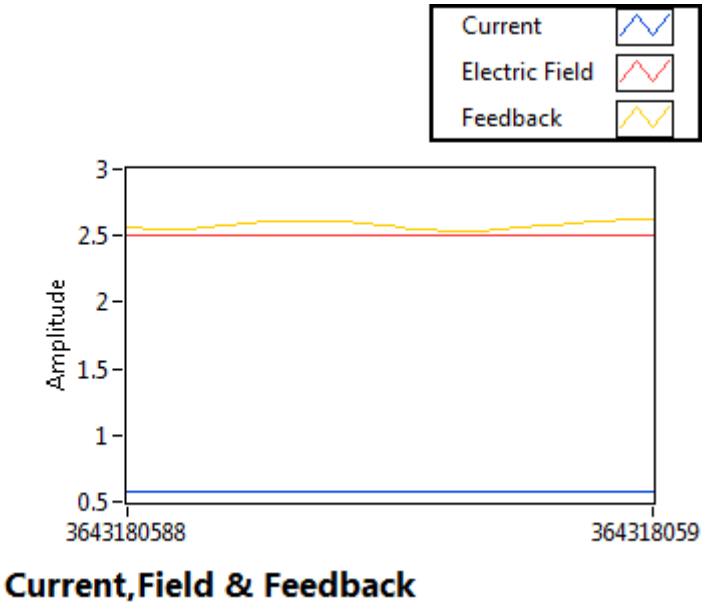

Fig 4.22: Feedback, Current and Electric field generated for 2nd alteration.

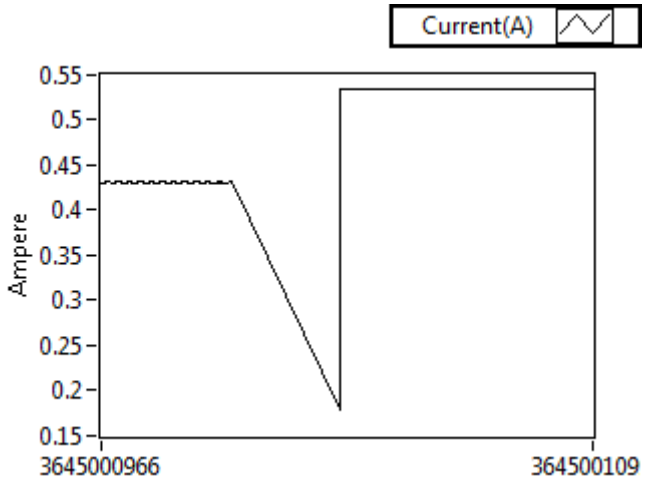

Fig 4.23: Current output for 2nd alteration.

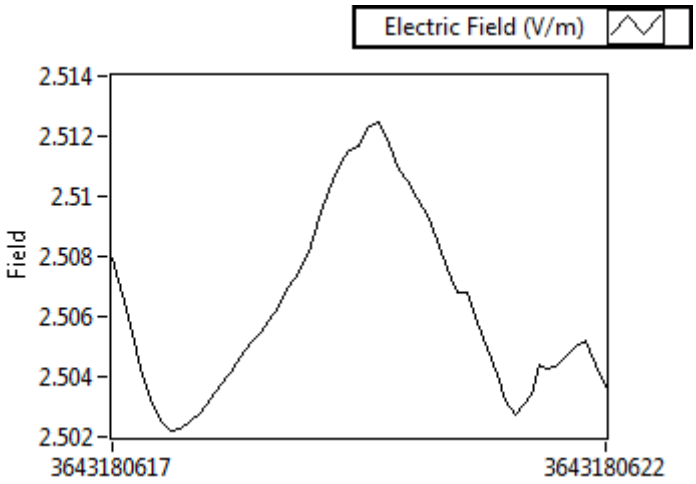

Fig 4.24: Electric field generated for 2nd alteration.

4.3.3. 3rd Alteration:

At the 3rd alteration/desired field of 3T was provided to the system. Fig. 4.26 shows the graph of required PFM to achieve desired field. Fig. 4.27 displays a graph obtained of the feedback, current and electric field generated against the desired field. The graph illustrates that the measured/output field came out to be 2.9992T when the input of 3T was given to the system.

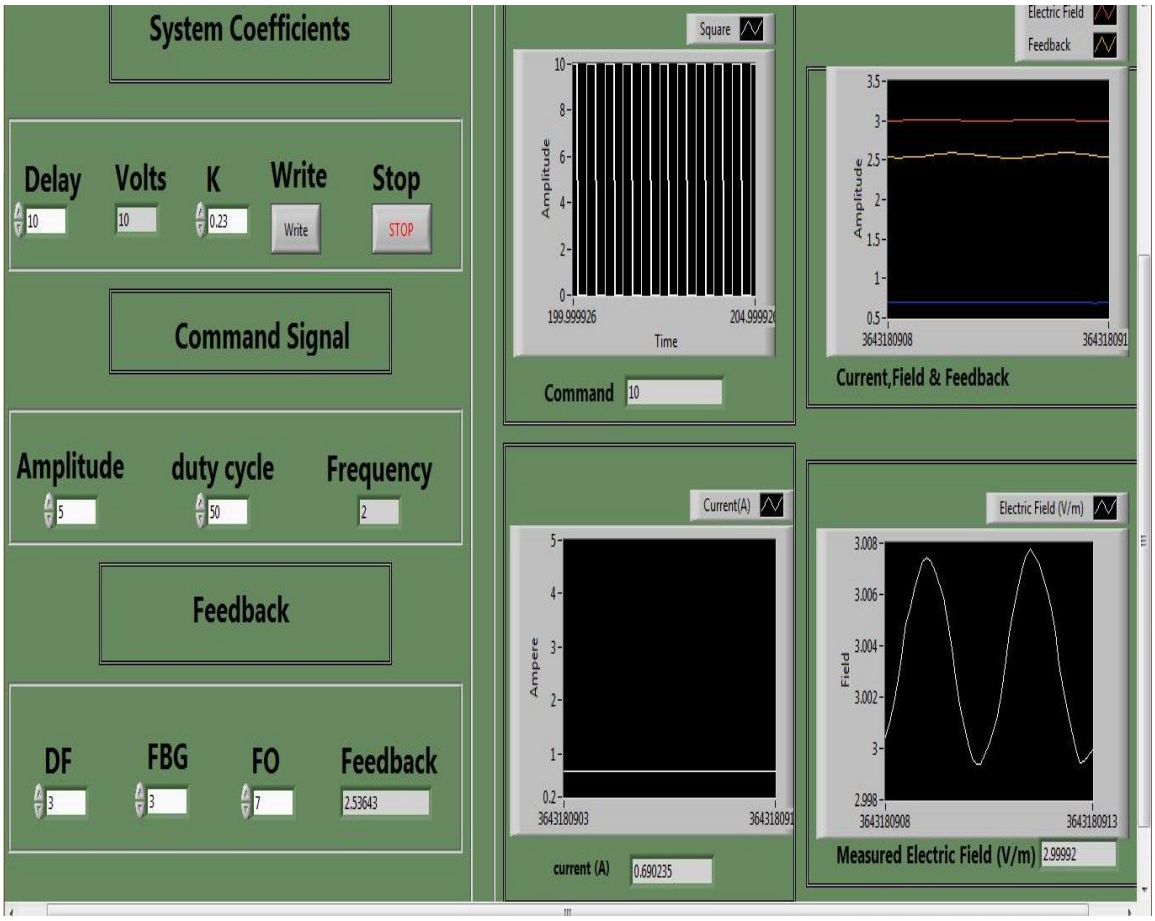

Fig 4.25: Complete system parameters and flow of the system (PFM)

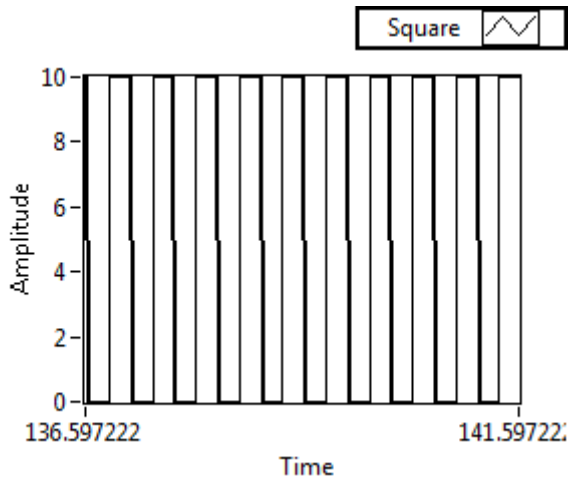

Fig 4.26 : PFM Command Graph for the 3rd alteration.

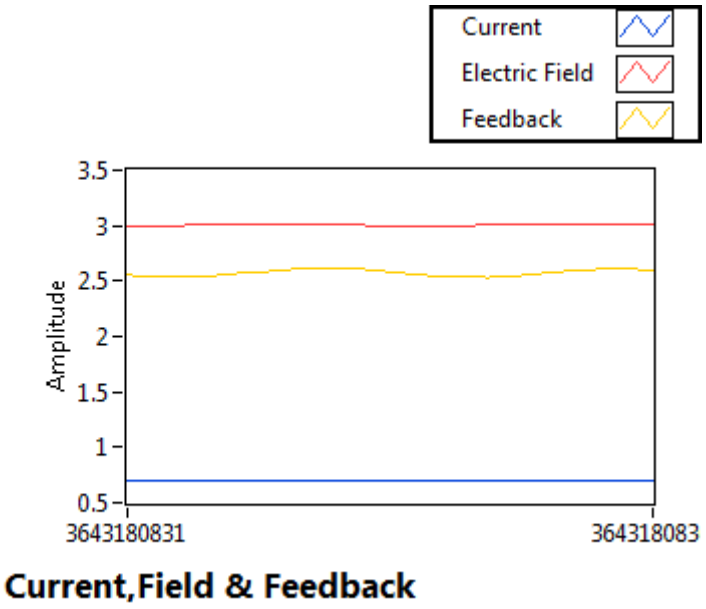

Fig 4.27: Feedback, Current and Electric field generated for 3rd alteration.

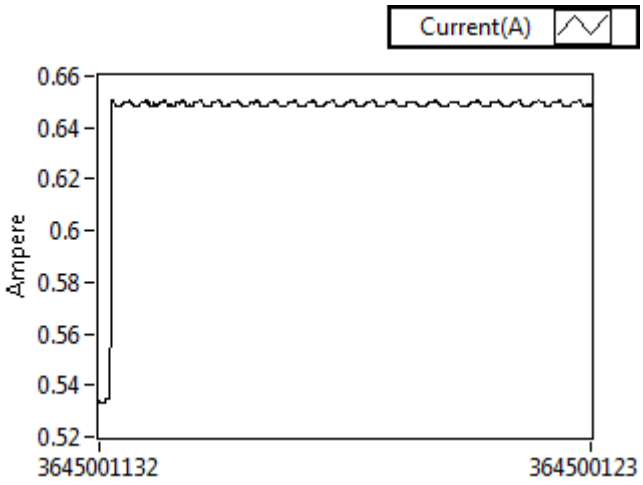

Fig 4.28: Current output for 3rd alteration.

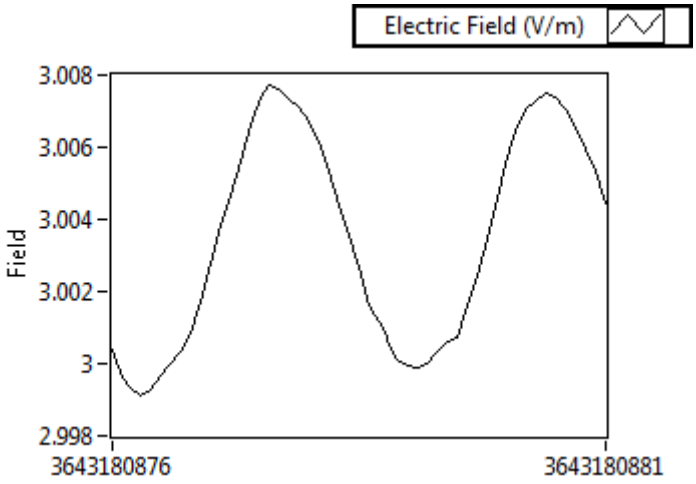

Fig 4.29: Electric field generated for 3rd alteration.

4.3.4. 4th Alteration:

At the 4th alteration/desired field of 3.5T was provided to the system. Fig. 4.31 shows the graph of required PFM to achieve desired field. Fig. 4.32 displays a graph obtained of the feedback, current and electric field generated against the desired field. The Fig 4.34 graph illustrates that the measured/output field came out to be 3.55036T when the input of 3.5T was given to the system.

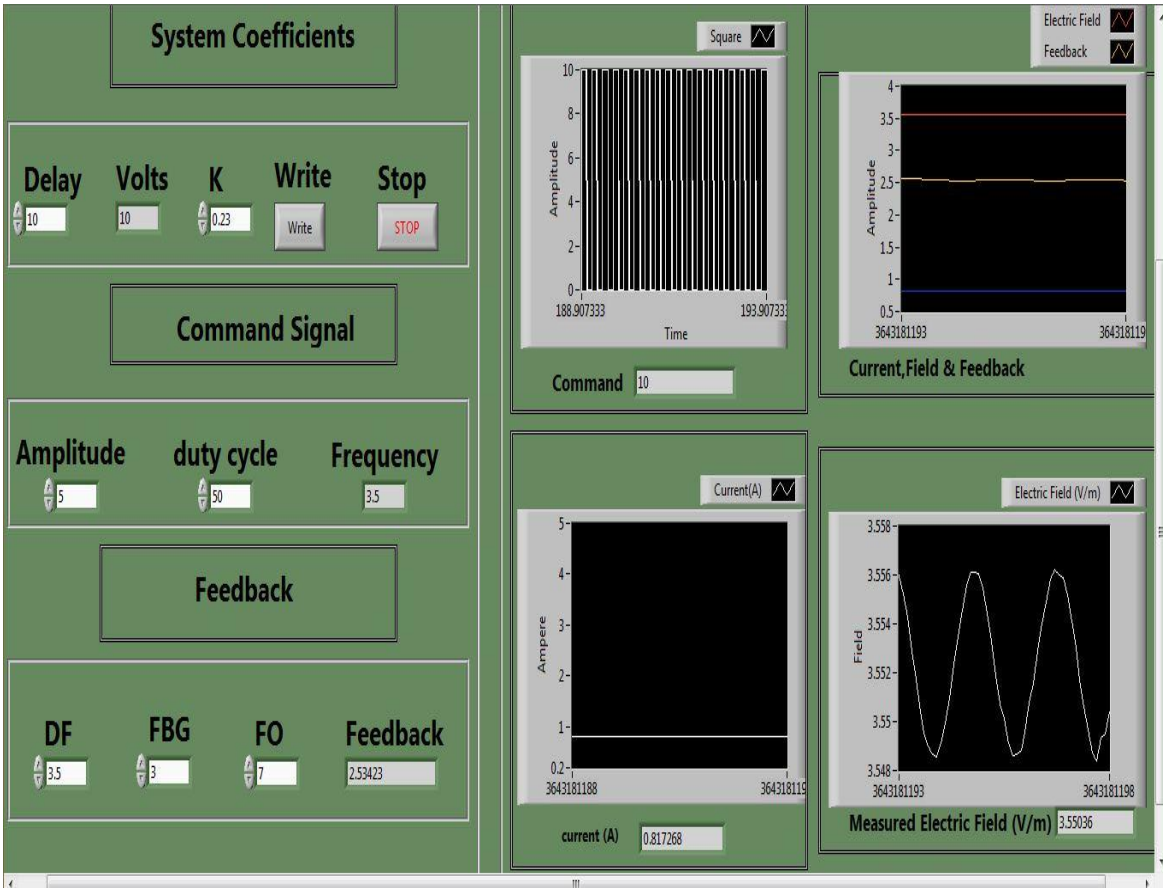

Fig 4.30: Complete system parameters and flow of the system (PFM)

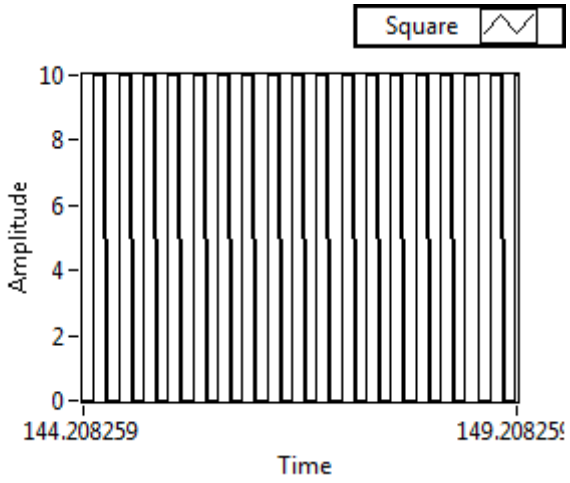

Fig 4.31 : PFM Command Graph for the 4th alteration.

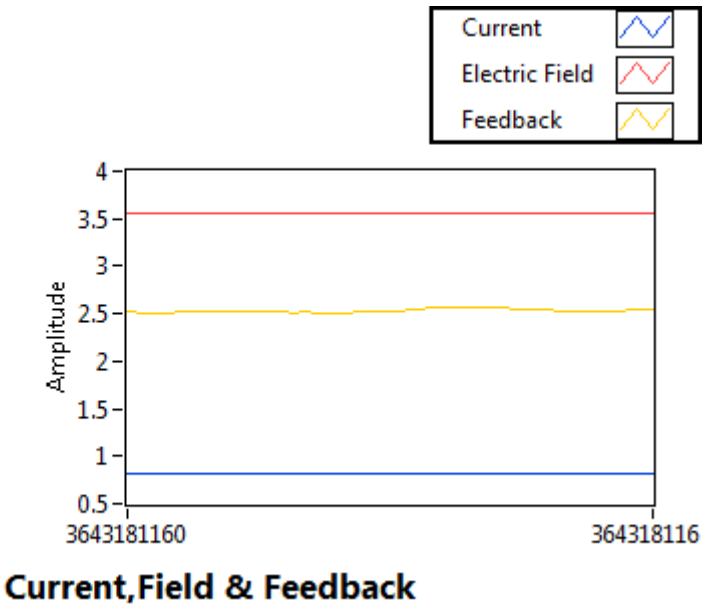

Fig 4.32: Feedback, Current and Electric field generated for 4th alteration.

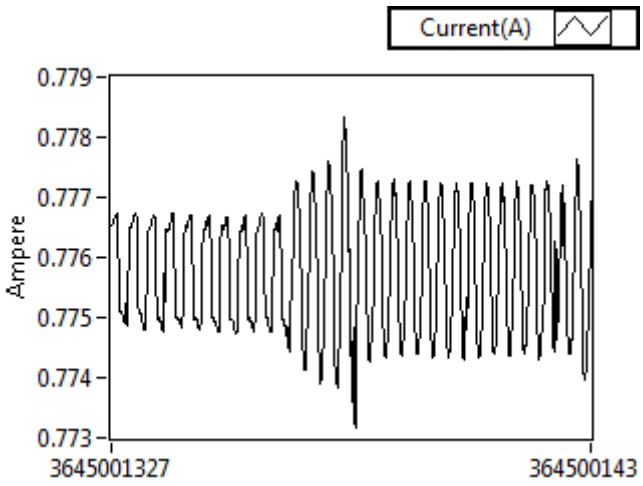

Fig 4.33: Current output for 4th alteration.

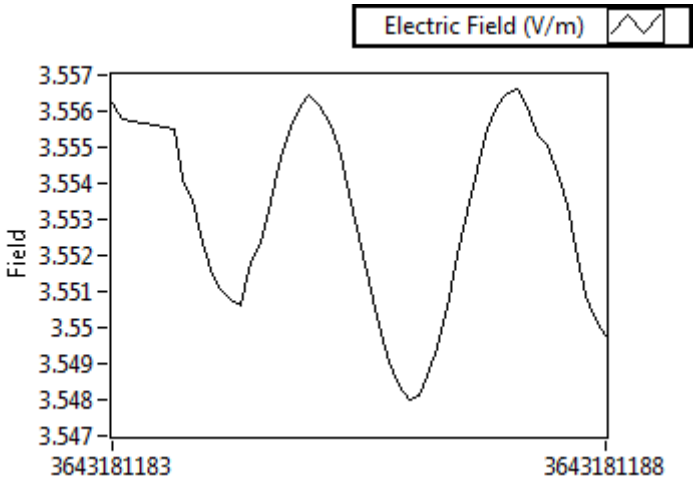

Fig 4.34: Electric field generated for 4th alteration.

4.3.5. 5th Alteration:

At the 5th alteration/desired field of 4T was provided to the system. Fig. 4.36 shows the graph of required PFM to achieve desired field. Fig. 4.37 displays a graph obtained of the feedback, current and electric field generated against the desired field. The Fig 4.39 graph illustrates that the measured/output field came out to be 4.04906T when the input of 4T was given to the system.

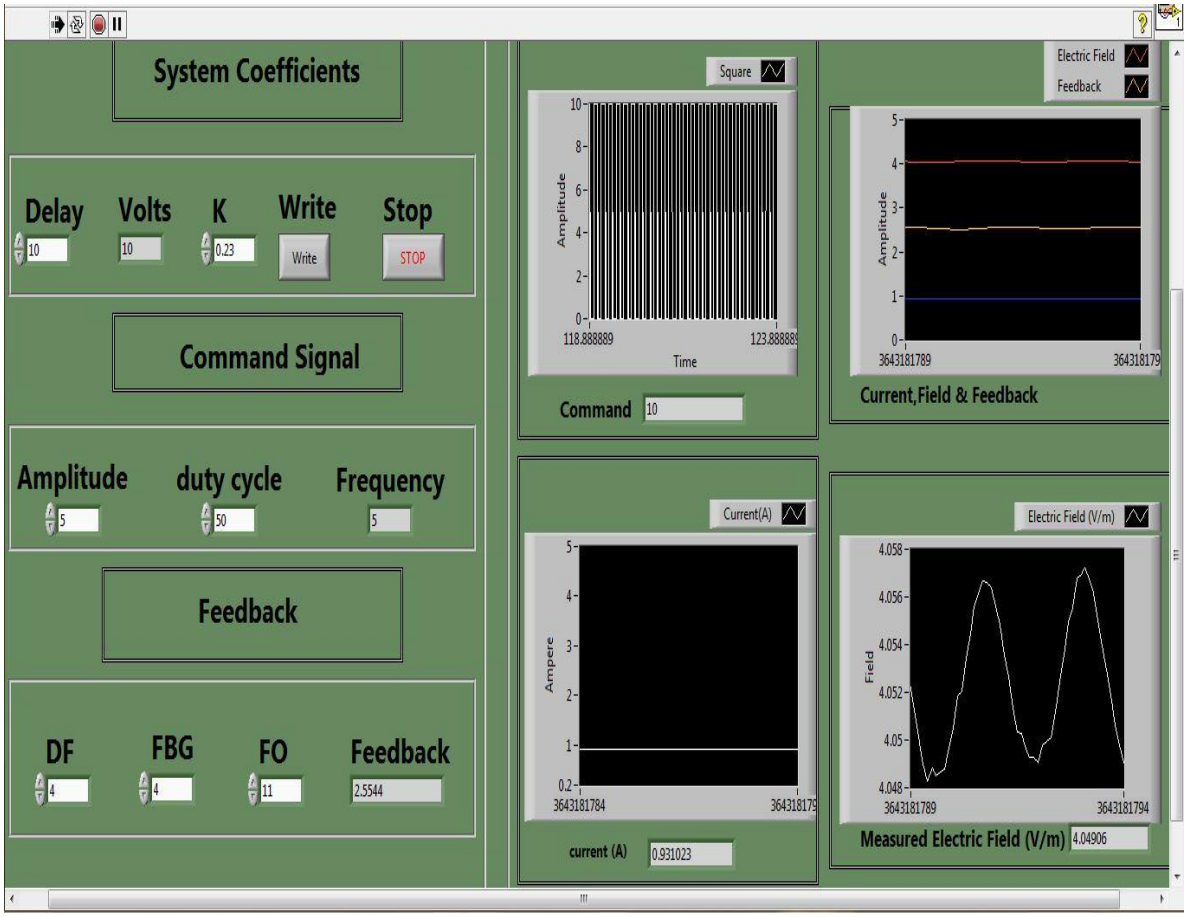

Fig 4.35: Complete system parameters and flow of the system (PFM)

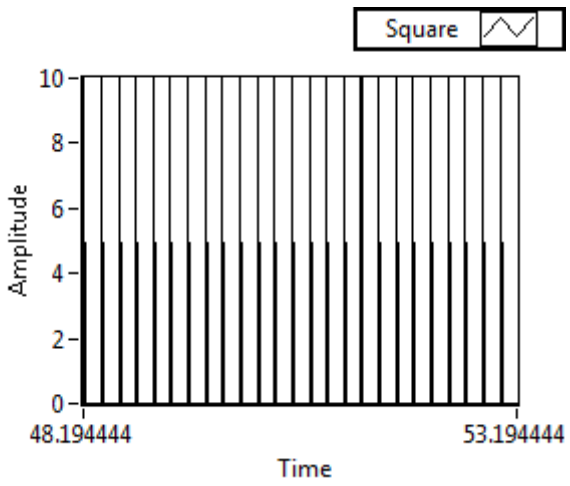

Fig 4.36: PFM Command Graph for the 5th alteration.

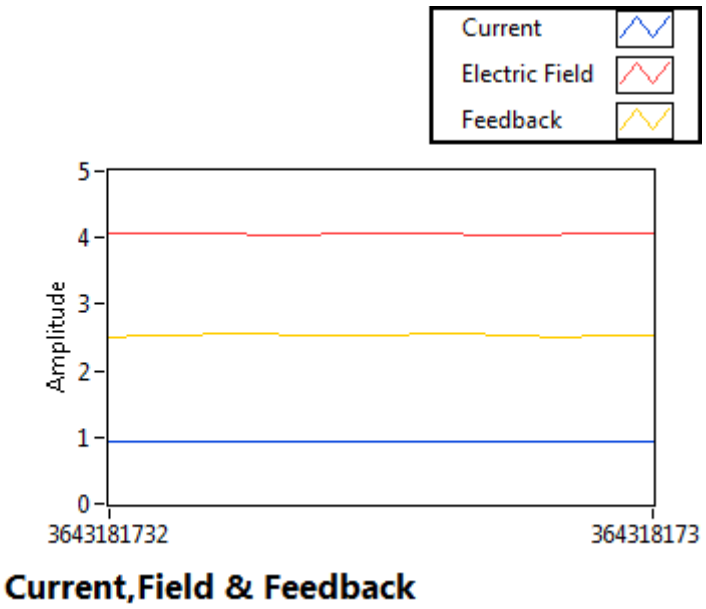

Fig 4.37: Feedback, Current and Electric field generated for 5th alteration.

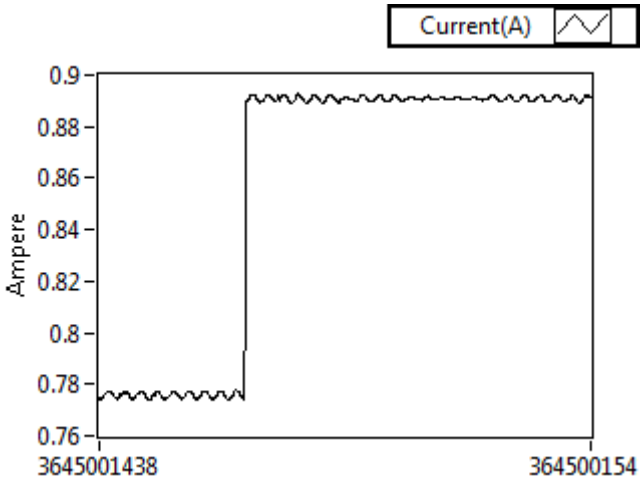

Fig 4.38: Current output for 5th alteration.

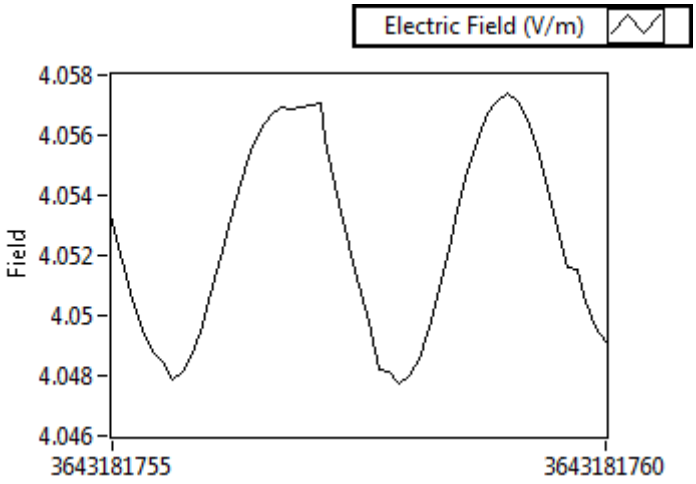

Fig 4.39: Electric field generated for 5th alteration.

4.3.6. 6th Alteration:

At the 6th alteration/desired field of 4.5T was provided to the system. Fig. 4.41 shows the graph of required PFM to achieve desired field. Fig. 4.42 displays a graph obtained of the feedback, current and electric field generated against the desired field. The fig 4.44 graph illustrates that the measured/output field came out to be 4.55127T when the input of 4.5T was given to the system.

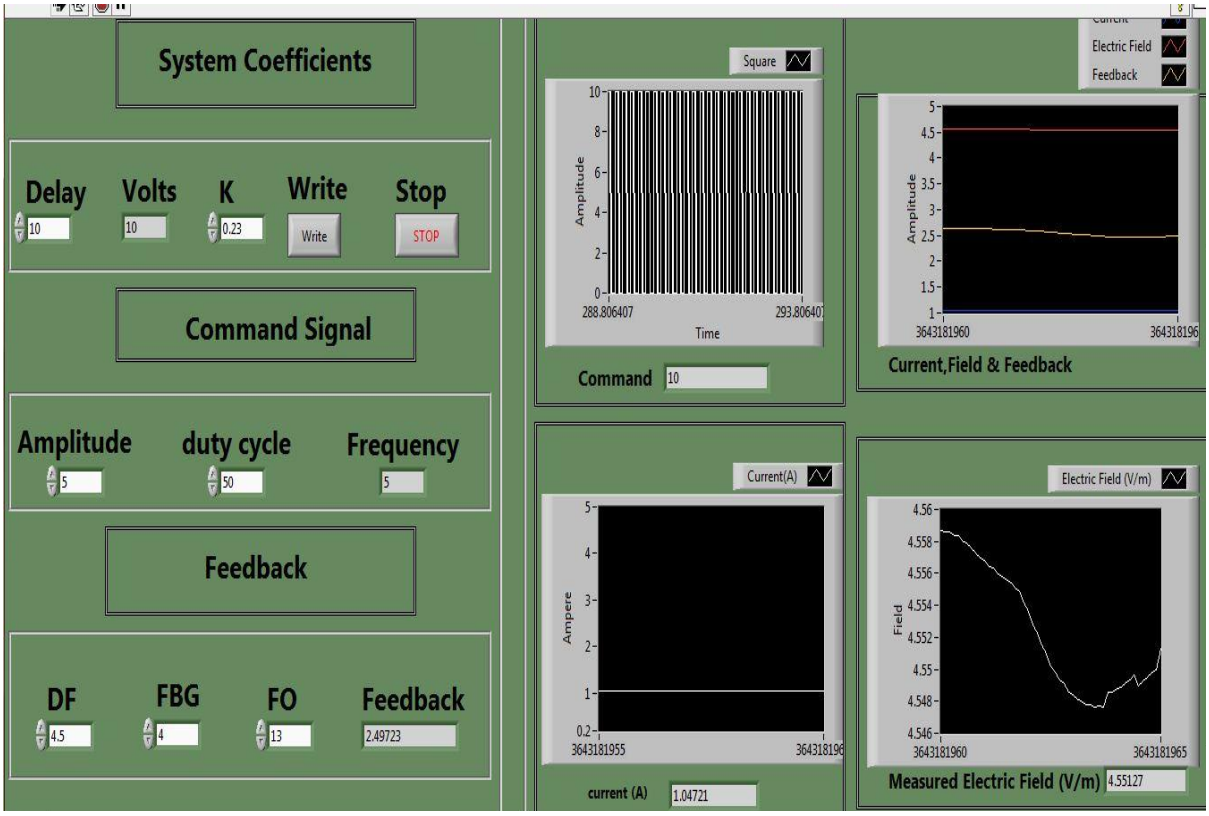

Fig 4.40: Complete system parameters and flow of the system (PFM)

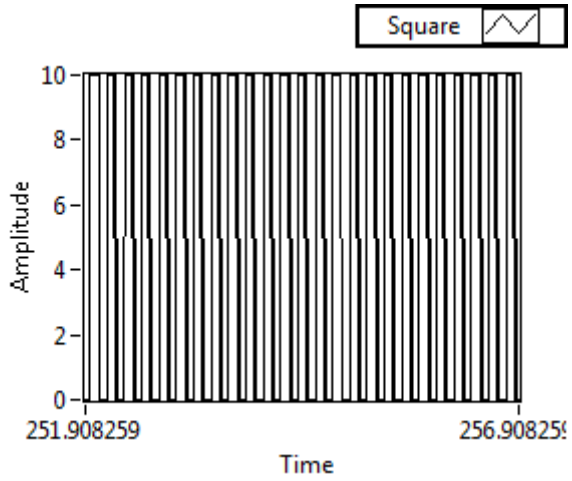

Fig 4.41 : PFM Command Graph for the 6th alteration.

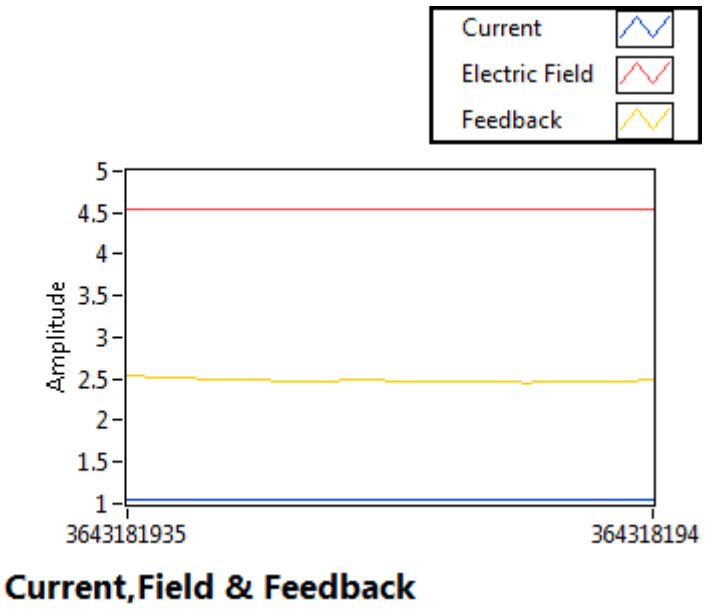

Fig 4.42 Feedback, Current and Electric field generated for 6th alteration.

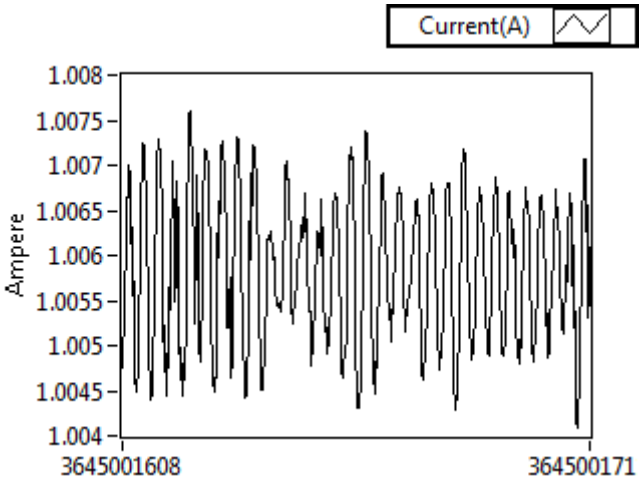

Fig 4.43: Current output for 6th alteration.

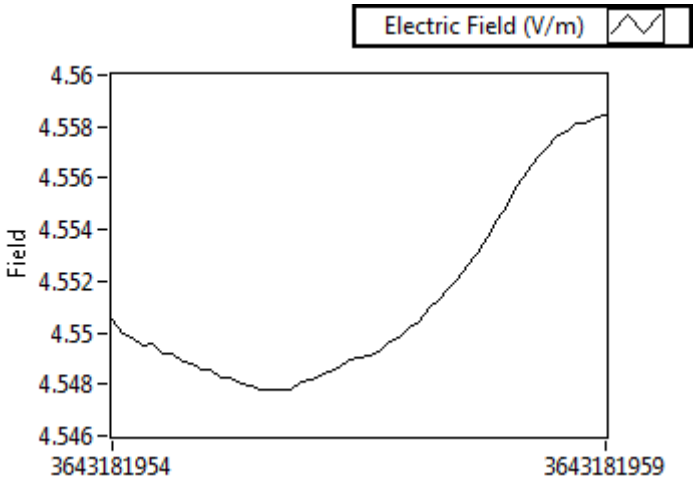

Fig 4.44: Electric field generated for 6th alteration.

4.3.7. 7th Alteration:

At the 7th alteration/desired field of 5T was provided to the system. Fig. 4.46 shows the graph of required PFM to achieve desired field. Fig. 4.47 displays a graph obtained of the feedback, current and electric field generated against the desired field. The fig 4.49 graph illustrates that the measured/output field came out to be 5.03275T when the input of 5T was given to the system.

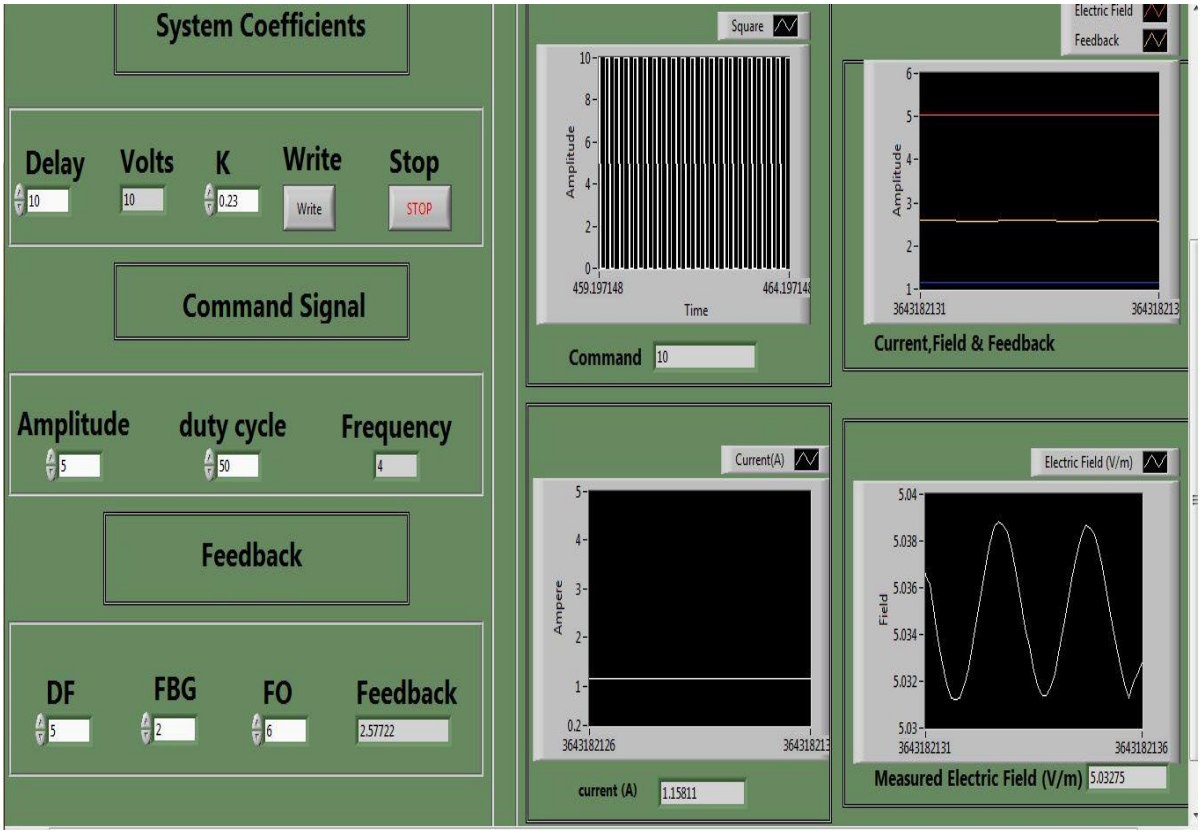

Fig 4.45: Complete system parameters and flow of the system (PFM)

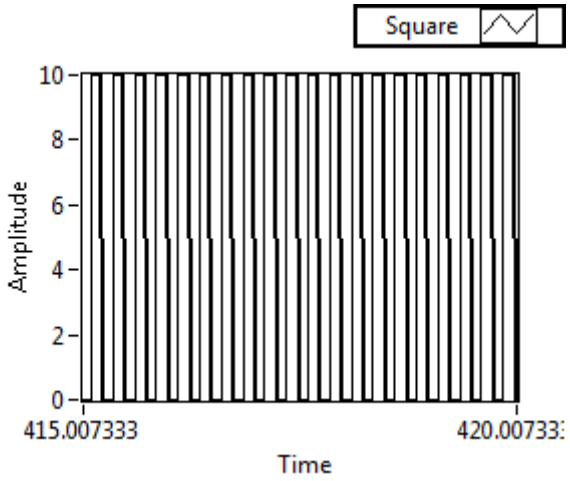

Fig 4.46 : PFM Command Graph for the 7th alteration.

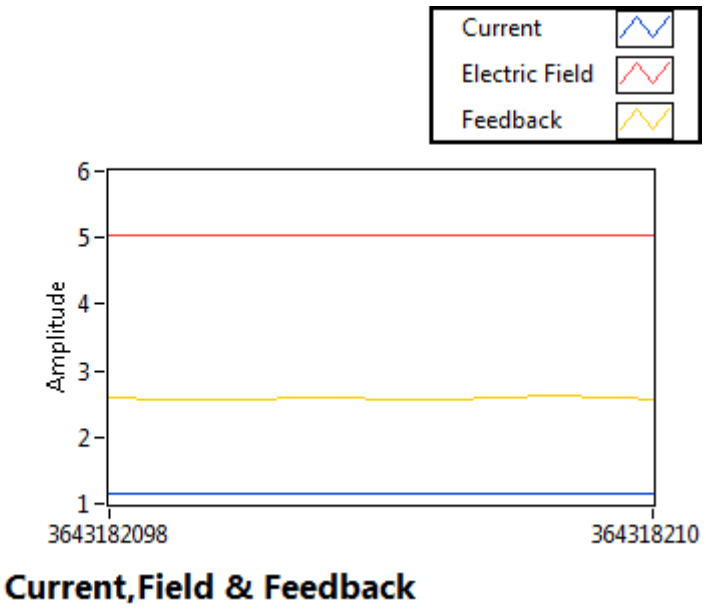

Fig 4.47: Feedback, Current and Electric field generated for 7th alteration.

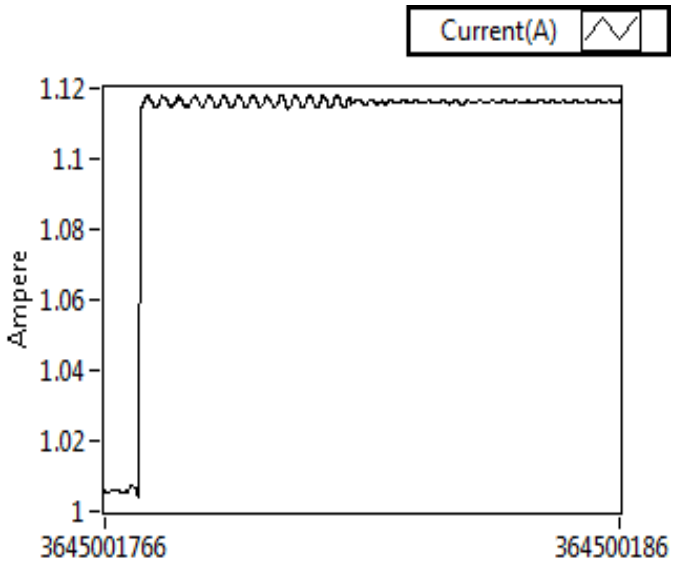

Fig 4.48: Current output for 7th alteration.

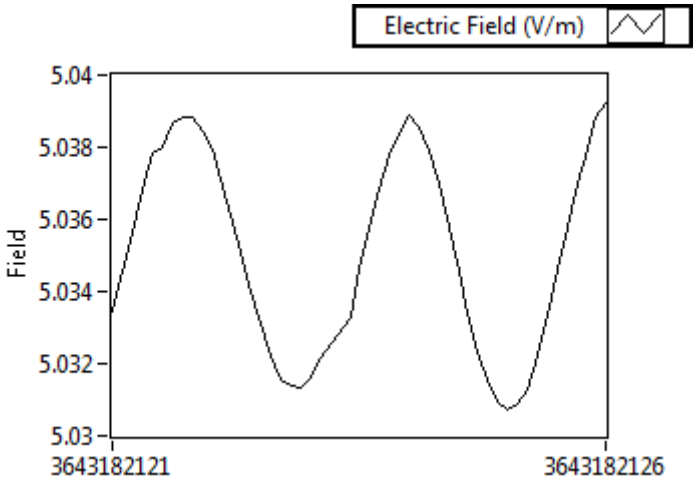

Fig 4.49: Electric field generated for 7th alteration.

Sr no	Desired Field, DF (Tesla)	Fuzzy based Set of Set of Membership Functions			Measured Field (Tesla)	Error
		1. Amplitude (V)	2. Frequency (KHz)	3. Duty Cycle (%)		
1	2	10	1	50	2.05674	0.05674
2	2.5	10	1.5	50	2.51094	0.01094
3	3	10	2	50	2.99992	0.00008
4	3.5	10	3.5	50	3.55036	0.05036
5	4	10	5	50	4.04906	0.04906
6	4.5	10	5	50	4.55127	0.05127
7	5	10	4	50	5.03275	0.03275

Table. 4.2: Summary of Fuzzy based Membership Functions with Measured Field and Error based on PFM.

Graph 4.50 represents relationship between desired EF and measured EF. The accuracy is improved with PFM technique by incorporating HFO.

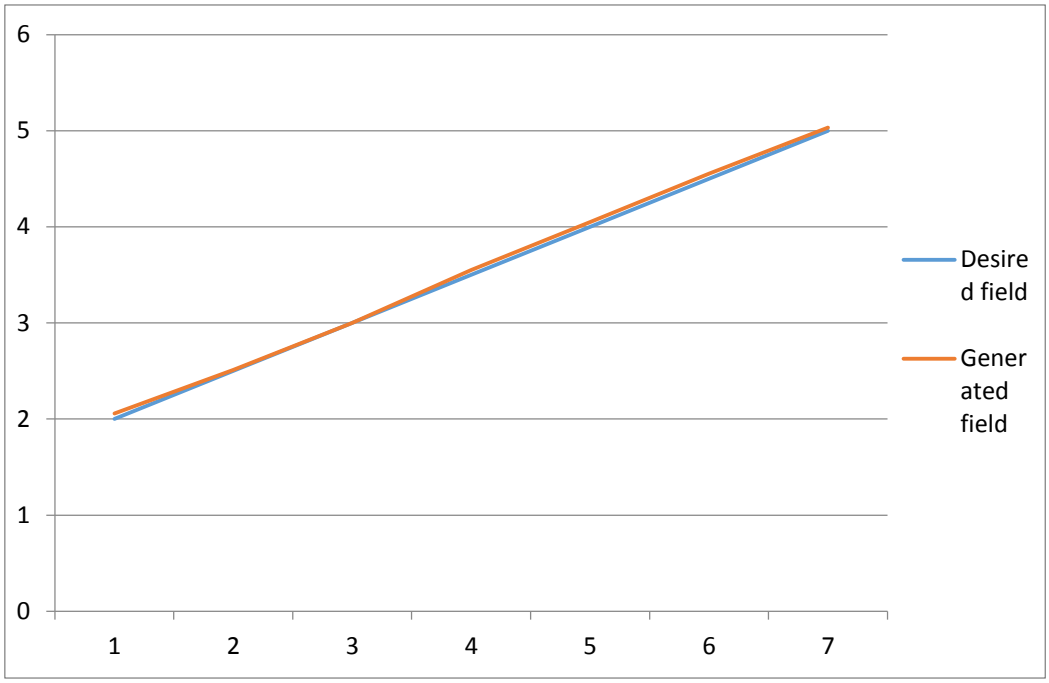

Fig 4.50: Graph representing relationship between desired EF and generated EF.

Chapter 5

Conclusions and Future Work

CHAPTER 5: CONCLUSIONS AND FUTURE WORK

Fuzzy based feedback controlled variable Electric Field system using HFO is designed with the capabilities of measuring, monitoring and controlling the electric field produced through the proposed designed and developed system. First PWM technique is used, results were analysed and studied which revealed system can generate the fields up to 2.5T effectively. Later on this technique is modified with PFM which increased span of generating EF from 2T to 5T. Fuzzy logic and HFO design drastically improve the stability and response of the system which can be seen in results of the simulations. EF of range 2T to 5T can be generated effectively from this system.

More over while comparison between previous researches it is noticed that our system is more accurate, robust and fully controlled compared to van de Graff generator and pulse generator discussed in literature review. The proposed system has a user interface which allows our system to be implemented in dynamic environments and industrial applications.

The system was validated/tested as can be seen from the results. Graphical results obtained illustrate that the electric fields were generated to a great accuracy.

This research presents numerous future prospects. In future this system can be optimized and mounted on a robotic arm module for smart contactless gripper. It will

be used to levitate non-metallic objects having different weights and sizes through auto adjustment of the electric fields which is required for various industrial operations. The same electric field can be setup to generate ionization in non-metallic objects. Afterwards the system shall be able to control the field adaptively during levitation as well as during the entire trajectory of the robotic arm's movement by countering all the dynamic variables during the entire trajectory of robotic arm by keeping the object levitating.

REFERENCES

[1] (2019, May) wikipedia. [Online]. https://en.wikipedia.org/wiki/Tesla_coil

[2] (2019, May) wikipedia. [Online]. https://en.wikipedia.org/wiki/Van_de_Graaff_generator

[3] R. J., K. T. Compton, and L. C. Van Atta, ""The Electrostatic Production of High Voltage for Nuclear Investigations"," p. Pg43.149V , February 1933.

[4] Boca Raton, "Van de Graaff's Generator," in *Electrical Engineering Handbook*. Florida USA, Florida USA, 1993, pp. ISBN 0-8493-0185-8.

[5] D. S. Jayas and R. A. Holley S. Jeyamkondan, "Pulsed electric field processing of foods: a review," *S. Jeyamkondan, D. S. Jayas and R. A. Holley, "Pulsed electric Journal of food protection* , vol. vol. 62, pp. , pp. 1088-1096, 1999, 1999.

[6] Song, et al. Yue, "“Electrostatic field simulation of variable pitch helical cathode.," in *Millimeter, and Terahertz waves*, 2014, pp. 2014 39th International Conference on Infrared, Millimeter, and Terahertz waves (IRMMW-THz).

[7] Linsa M, and Resmi R L,". “Analysis of variable substrate properties effects on electric field distribution in MEMS EVA tunable filters.," in *2015 International Conference on Control, Instrumentation, Communication and Computational Technologies* , 2011.

[8] H., et al. Yotsuyanagi, "“Random pattern testability of the open defect detection method using application of time-Variable electric field.”, ," in *Proceedings First IEEE International Workshop on Electronic Design, Test and Applications 2002*, pp. doi:10.1109/delta.2002.

[9] S. Jeyamkondan, D. S. Jayas, and R. A. Holley, "Pulsed electric field processing of foods: a review," *Journal of food protection*, vol. 62, pp. 1088-1096, 1999.

[10] T. B. Jones and J. P. Kraybill, ""Active feedback-controlled dielectrophoretic levitation".," *Journal of applied physics, ,* vol. vol. 60, pp. , pp. 1247-1252, 1986.

[11] T. B. Jones and J. P. Kraybill, "Active feedback-controlled dielectrophoretic levitation," *Journal of applied physics*, vol. 60, pp. 1247-1252, 1986.

[12] M. Paraliev, C. Gough, and S. Ivkovic, "Tesla coil design for electron gun application," *IEEE Pulsed Power Conference*, pp. 1085-1088, 2005.

[13] Ronnie Ross et al., ""Underwater electric field measurement and analysis," ," *OCEANS--Anchorage, ,* pp. pp. 1-5., 2017.

[14] B. M. Novac, I. R. Smith, B. Lynn, and R. A. Miller, A. J. Young, ""Two-dimensional modelling of a double-spiral coil system for high electric field generation for biological applications,"., " *IET, 2001*.

[15] J. H. Woo, E. Y. Choi, and J. W. Wu, "Electric field control of Berry phase in an optical interferometer," in *Conference on Lasers and Electro-Optics/Pacific Rim*, 2009, p. TUP5_24.

[16] Badar Ali, Yasar Ayaz, Mohsin Jamil, Syed Omer Gilani, and Naveed Muhammad, "Improved method for stereo vision-based human detection for a mobile robot following a target person," *South African Journal of Industrial Engineering*, vol. 26, pp. 102-119, 2015.

[17] Badar Ali, Khawaja Fahad Iqbal, Yasar Ayaz, and Naveed Muhammad, "Human detection and following by a mobile robot using 3d features," in *Mechatronics and Automation (ICMA), 2013 IEEE International Conference on*, 2013, pp. 1714-1719.

[18] Badar Ali et al., "Human tracking by a mobile robot using 3D features," in *Robotics and Biomimetics (ROBIO), 2013 IEEE International Conference on*, 2013, pp. 2464-2469.

[19] Z. N. Zakaria, Thomas Andritsch, and P. L. Lewin, "Electric field measurement in liquid dielectrics using Kerr effect," in *Electrical Insulation and Dielectric Phenomenon (CEIDP), 2017 IEEE Conference on*, 2017, pp. 720-723.

[20] F. S. Mozer and R. Serlin, "Magnetospheric electric field measurements with balloons," *Journal of Geophysical Research*, vol. 74, pp. 4739-4754, 1969.

[21] Xavier Gonze, "First-principles responses of solids to atomic displacements and homogeneous electric fields: Implementation of a conjugate-gradient algorithm," *Physical Review B*, vol. 55, p. 10337, 1997.

[22] L. Richard Huang et al., "Generation of large-area tunable uniform electric fields in microfluidic arrays for rapid DNA separation," in *Electron Devices Meeting, 2001. IEDM'01. Technical Digest. International*, 2001, pp. 16-3.

[23] H. Ohno et al., "Electric-field control of ferromagnetism," *Nature*, vol. 408, p. 944, 2000.

[24] Shizhe Wu et al., "Electric-Field-Controlled Room Temperature AMR Switching in a NiFe/BiFeO 3/SrRuO 3/SrTiO 3 (111) Heterostructure," *IEEE Transactions on Magnetics*, vol. 11, pp. 1-3, 2015.

[25] Francisco J. Barba et al., "Current applications and new opportunities for the use of pulsed electric fields in food science and industry," *Food Research International*, vol. 77, pp. 773-798, 2015.

[26] Hajer Omrane, Mohamed Slim Masmoudi, and Mohamed Masmoudi, "Fuzzy logic based control for autonomous mobile robot navigation," *Computational intelligence and neuroscience*, vol. 2016, 2016.

[27] Snejana Yordanova, Daniel Merazchiev, and Lakhmi Jain, "A two-variable fuzzy control design with application to an air-conditioning system," *IEEE Transactions on fuzzy systems*, vol. 23, pp. 474-481, 2015.

[28] A. S. Ahmad et al., "A review on applications of ANN and SVM for building electrical energy consumption forecasting," *Renewable and Sustainable Energy Reviews*, vol. 33, pp. 102-109, 2014.

[29] Dhan Jeet Singh, Nishchal K. Verma, A. K. Ghosh, and Appasaheb Malagaudanvar, "Fuzzy systems practices for aerodynamic parameter modeling of the aircraft," in *Computer Applications In Electrical Engineering-Recent Advances (CERA), 2017 6th International Conference on*, 2017, pp. 462-467.

[30] Jingyu Liu, Wen Zhang, Xiaodong Chu, and Yutian Liu, "Fuzzy logic controller for energy savings in a smart LED lighting system considering lighting comfort and daylight," *Energy and Buildings*, vol. 127, pp. 95-104, 2016.

[31] R. S. S. Syamsul, "Control System Based on Fuzzy Logic in Nutmeg Oil Distillation Process for Energy Optimization," in *International Conference on Information and Communications Technology (ICOIACT)*, Yogyakarta, Indonesia, 2018.

[32] E. U. P. Febryan Hari Purwanto, "Design of Server Room Temperature and Humidity," in *International Conference on Information and Communications Technology (ICOIACT)*, Yogyakarta, Indonesia, 2018.

[33] D. P. Z. P. V. F. O. S. a. P. S. M. Fedorová, "The Fuzzy System as a Promising Tool for Drugs Selection in Medical Practice," in *IEEE Access. 1-1. 10.1109/ACCESS.2018.2831282*, 2018.

[35] Hiroyuki Yotsuyanagi, Masaki Hashizume, Taisuke Iwakiri, Masahiro Ichimiya, and Takeomi Tamesada, "Random pattern testability of the open defect detection method using application of time-variable electric field," in *Electronic Design, Test and Applications, 2002. Proceedings. The First IEEE International Workshop on*, 2002, pp. 387-391.

[36] R. ScHMIDT, "Electric field measurements on the G EOT AIL satellite," *J.*

Geomagn, 1994.

[37] Ronnie Ross et al., "Underwater electric field measurement and analysis," in *OCEANS--Anchorage, 2017*, 2017, pp. 1-5.

[38] A. J. Young, B. M. Novac, I. R. Smith, B. Lynn, and R. A. Miller, "Two-dimensional modelling of a double-spiral coil system for high electric field generation for biological applications," *IET*, 2001.

[39] Dapeng Zhang, Zhengtao Zhang, Qun Gao, De Xu, and Song Liu, "Development of a monolithic compliant SPCA-driven micro-gripper," *Mechatronics*, vol. 25, pp. 37-43, 2015. [Online]. http://www.sciencedirect.com/science/article/pii/S0957415814002062

[40] D. Vogtmann and S. Bergbreiter, "Magnetic actuation of ultra-compliant micro robotic mechanisms," in *2014 IEEE/RSJ International Conference on Intelligent Robots and Systems*, Sept 2014, pp. 809-815.

[41] Franziska Ullrich, Kanika S. Dheman, Simone Schuerle, and Bradley J. Nelson, "Magnetically actuated and guided milli-gripper for medical applications," in *Robotics and Automation (ICRA), 2015 IEEE International Conference on*, 2015, pp. 1751-1756.

[42] Tomokazu Takahashi, Masato Suzuki, and Seiji Aoyagi, "Octopus bioinspired vacuum gripper with micro bumps," in *Nano/Micro Engineered and Molecular Systems (NEMS), 2016 IEEE 11th Annual International Conference on*, 2016, pp. 508-511.

[43] R. Sudhakar, R. Shanu Prathap, K. Sudarshan, and S. Vijay, "Literature Review on Micro Grippers," *International Journal of Emerging Trends in Engineering and Development*, vol. 6, pp. 59-74, 2016.

[44] Michael Schilp, Josef Zimmermann, and Adolf Zitzmann, Vacuum gripper, #feb#~23 2016, US Patent 9,266,686.

[45] C. Pacchierotti et al., "Steering and Control of Miniaturized Untethered Soft Magnetic Grippers With Haptic Assistance," *IEEE Transactions on Automation Science and Engineering*, vol. PP, pp. 1-17, 2017.

[46] Michael O. Obaji and Shiwu Zhang, "Investigation into the force distribution mechanism of a soft robot gripper modeled for picking complex objects using embedded shape memory alloy actuators," in *Robotics, Automation and Mechatronics (RAM), 2013 6th IEEE Conference on*, 2013, pp. 84-90.

[47] T. Nishimura, K. Mizushima, Y. Suzuki, T. Tsuji, and T. Watanabe, "Variable-Grasping-Mode Underactuated Soft Gripper With Environmental Contact-Based Operation," *IEEE Robotics and Automation Letters*, vol. 2, pp. 1164-1171, April 2017.

[48] Sandeep Krishnan and Laxman Saggere, "Design and development of a novel micro-clasp gripper for micromanipulation of complex-shaped objects," *Sensors and Actuators A: Physical*, vol. 176, pp. 110-123, 2012. [Online]. http://www.sciencedirect.com/science/article/pii/S0924424711005449

[49] Hyun-Wook Kang, In Hwan Lee, and Dong-Woo Cho, "Development of a micro-bellows actuator using micro-stereolithography technology," *Microelectronic Engineering*, vol. 83, pp. 1201-1204, 2006, Micro- and Nano-Engineering MNE\ 2005Proceedings of the 31st International Conference on Micro- and Nano-Engineering. [Online]. http://www.sciencedirect.com/science/article/pii/S0167931706002486

[50] Ravi K. Jain, Somajoyti Majumder, Bhaskar Ghosh, and Surajit Saha, "Design and manufacturing of mobile micro manipulation system with a compliant piezoelectric actuator based micro gripper," *Journal of Manufacturing Systems*, vol. 35, pp. 76-91, 2015. [Online]. http://www.sciencedirect.com/science/article/pii/S0278612514001472

[51] R. K. Jain, S. Majumder, and A. Dutta, "SCARA\ based peg-in-hole assembly

using compliant IPMC\ micro gripper," *Robotics and Autonomous Systems*, vol. 61, pp. 297-311, 2013. [Online]. http://www.sciencedirect.com/science/article/pii/S0921889012002229

[52] R. K. Jain, S. Datta, and S. Majumder, "Design and control of an IPMC\ artificial muscle finger for micro gripper using EMG\ signal," *Mechatronics*, vol. 23, pp. 381-394, 2013. [Online]. http://www.sciencedirect.com/science/article/pii/S0957415813000408

[53] Katerina Ivanova et al., "Thermally driven microgripper as a tool for micro assembly," *Microelectronic Engineering*, vol. 83, pp. 1393-1395, 2006, Micro- and Nano-Engineering MNE\ 2005Proceedings of the 31st International Conference on Micro- and Nano-Engineering. [Online]. http://www.sciencedirect.com/science/article/pii/S0167931706000943

[54] A. Ichikawa, S. Sakuma, T. Shoda, F. Arai, and S. Akagi, "On-chip enucleation of oocyte using untetherd micro-robot with gripping mechanism," in *MHS2013*, Nov 2013, pp. 1-3.

[55] Yufei Hao et al., "Universal soft pneumatic robotic gripper with variable effective length," in *Control Conference (CCC), 2016 35th Chinese*, 2016, pp. 6109-6114.

[56] Gen Endo and Nobuhiro Otomo, "Development of a food handling gripper considering an appetizing presentation," in *Robotics and Automation (ICRA), 2016 IEEE International Conference on*, 2016, pp. 4901-4906.

[57] C. H. Chen and W. d. Chong, "Force controlled robot gripper with flexible joint for delicate assembly task," in *2013 13th International Conference on Control, Automation and Systems (ICCAS 2013)*, Oct 2013, pp. 935-939.

[58] A. Alogla, F. Amalou, P. Scanlan, W. Shu, and R. L. Reuben, "Development of a Pneumatically Actuated Cantilever Based Micro-tweezer," *Procedia Engineering*, vol. 87, pp. 1390-1393, 2014. [Online].

http://www.sciencedirect.com/science/article/pii/S1877705814028240

[59] A. S. Ahmad et al., "A review on applications of ANN and SVM for building electrical energy consumption forecasting," *Renewable and Sustainable Energy Reviews*, vol. 33, pp. 102-109, 2014.

Appendices

APPENDIX A.

Appendix A: List of Abbreviations

SSD: Solid State

DAQ: Data Acquisition

NI: National Instruments

PWM: Pulsed Width Modulation

S/N: Signal to Noise Ratio

IC: Integrated Circuit

APPENDIX B: LIST OF COMPONENTS

1. NI USB DAQ 6001
2. SSD Tesla Coil
3. ACS 712x30A Sensor Module (Hall Effect Sensor)
4. 12 Volt Power Supply

APPENDIX C: LIST OF SOFTWARE

1. NI LabVIEW 2014
2. NI MAX
3. Proteus 8 Professional

APPENDIX D: DATASHEETS OF CORE COMPONENTS

ACS 712x30A Sensor Module

Characteristic	Symbol	Test Conditions	Min.	Typ.	Max.	Units
Optimized Accuracy Range	I_P		–30	–	30	A
Sensitivity	Sens	Over full range of I_P, T_A = 25°C	63	66	69	mV/A
Noise	$V_{NOISE(PP)}$	Peak-to-peak, T_A = 25°C, 66 mV/A programmed Sensitivity, C_F = 47 nF, C_{OUT} = open, 2 kHz bandwidth	–	7	–	mV
Zero Current Output Slope	$\Delta V_{OUT(Q)}$	T_A = –40°C to 25°C	–	–0.35	–	mV/°C
		T_A = 25°C to 150°C	–	–0.08	–	mV/°C
Sensitivity Slope	ΔSens	T_A = –40°C to 25°C	–	0.007	–	mV/A/°C
		T_A = 25°C to 150°C	–	–0.002	–	mV/A/°C
Total Output Error[2]	E_{TOT}	I_P = ±30 A, T_A = 25°C	–	±1.5	–	%

NI USB DAQ 6001

Characteristic	Value
Input Range	± 10 V
Working Voltage	± 10 V
Input voltage Range	0 – 5 V
Output Voltage	5 V
Maximum Current	150 mA
Short circuit Current	50 mA
USB bus Speed	12mb/s
Digital Input Output Channels	13
Analog Input Channels	8
Analog Output Channels	2

APPENDIX E: PIN CONFIGURATION OF CORE COMPONENTS

ACS 712x30A Sensor Module

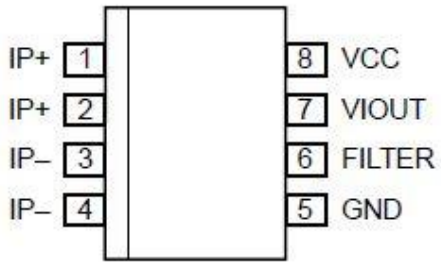

NI USB DAQ 6001